Authors' point-by-point responses to Reviewers' recommendations

We thank the reviewers for the time spent reading our manuscript and for their constructive comments and suggestions. We greatly appreciate all feedback provided. All comments are addressed as completely as possible below. The revised manuscript is attached as a pdf file with all changes tracked. In the following text, the particular concerns/comments raised by the Reviewer no.2 are presented in *italic*, whereas our responses are in **bold**.

Response to Reviewer no. 2: Prof. Giorgio Ghiglieri

1.

This paper discusses the re-processing of regional-scale airborne electromagnetic data that is used in building a 3D geological model of the Nasia Sub-basin, Northern Ghana. The authors, using and exploiting data from other studies and surveys, propose a geological model aimed both at new important knowledge strictly geological and stratigraphic, but above all they propose a new hydrogeological model aimed at finding groundwater resources. The overall objective of the research is to develop a decision support tool for understanding groundwater occurrence to facilitate efficient development and optimization of the water resources in the area. Therefore, this paper has a high scientific level because of the amount of data presented, the complexity of the discussion and, last but not least, its potential application to water resources management. Its understanding in the appropriate geological context may provide criteria for water management in the area and to reduce drought risk/processes. In addition, the proposed methodology can be strategic in areas such as these where data availability is scarce and logistic difficult.

We appreciate the overall positive opinion of Prof. Ghiglieri concerning our manuscript. In particular, we are happy for his acknowledgement: (i) of the amount of data (and data kinds) we handled and (ii) of the complexity of the research we performed.
We really hope this study can have significant impacts on the development of groundwater resources in the area.

2.

Nevertheless, there are some details that, in my opinion, may improve the quality of the presented data as well as the clarity of the text. Those are the following. The paper is quite concise and correctly organized. In the introduction section, add some "state of the art".

The "Introduction" has been shortened in agreement with the indications of Reviewer no. 1. Moreover, we included a very short description of the overall geological framework in the area. However, we feel that adding further details about the state-of-the-art in that section would not be very effective as the current knowledge about the different aspects of the proposed research is already detailed in the different, specific, sections of the paper.

3.

Data and methods are sound and convincing. But, I would have expected to see borehole stratigraphic logs. The authors claim to have used logs for geophysical calibration as well.

In the revised version of the manuscript, we included the new Fig. R2.1 showing two examples of the boreholes used (together with other sources of information) for the interpretation of the geophysical resistivity models. Those wells were the closest to the flight lines of the geophysical survey (so, to some extent, the most significant in this respect).
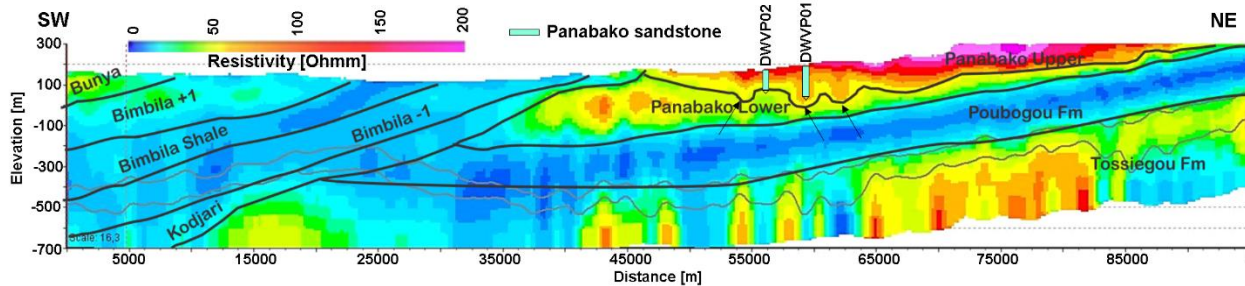
Figure R2.1: Cross-section along SW-NE line 2 across the study area (see Fig. 1a for the location) with the conceptual geological interpretations showing the U-shaped valleys (from about 53 km to 63 km). In addition, also two of the geologic logs (DWVP02 and DWVP01 – Fig. 1a) used for demarcation of lithostratigraphic boundaries and the interpretation/verification of the geophysical model are shown. The two solid grey lines at the bottom represents the DOIs. The three arrows indicate the location of the paleovalleys.

4.

Honestly, I had some problems reading the conceptual model in Fig 1b. Fig. 1 a is not really clear. I suggest at least change the legend using the international standard of geological legend.

In the new version, accordingly to the remarks from the Reviewers, we largely modified Fig.s 1a and 1b (in this respect, please, see Fig. R2.2, here). We believe that, in the revised manuscript, the legend, and, in general, the figure, are much clearer.

5.

If there are hydrological data also from previous studies, it would be very useful to describe them and insert them in Fig.1 and 1b, so readers begin to understand which aquifers aquiclude or aquitard are.

Even though the final goal of the project is to use the geological model for hydrogeological purposes, we believe that the manuscript is already quite complex and rich of different kinds of information.
For these reasons, we feel that the additional details suggested by the Reviewer might be, not only out of the scope of the paper, but, also, potentially distracting for the readers.

6.

The results and discussions are really interesting, but I suggest to change it up a bit. In my opinion, the geological and hydrogeological context will be better clarified. Moreover, please use the use the chronostratigraphic method (from oldest to newest or viceversa); same symbols and colors in all figures, etc. better explain the hydrogeological interpretation (acquifer, aquicludes, etc).

Concerning the more hydrogeological remarks, we provided our perspective at point *5.*, in the present document. Regarding the homogenization of the color scales in the figures, we definitely agree with the Reviewer and we modified the manuscript accordingly. The same is now true also for the chronostratigraphic order (the oldest located at the bottom). See, for example, the new Fig.s 1 and 6, in the revised manuscript (here, Fig.s R2.2 and R2.3).

7.

If it is possible, better clarify the geometry of the paleovalleys in hydrogeological terms and according to this new model we can hypothesize the potential of the aquifer? Last doubt, do we have data on quality?

We further clarified the orientation and geometry of the paleovalleys through the inclusion of the new Fig. 9 (here, Fig. R2.4) and the associated discussion.
However, the potential of the aquifer is still under investigation and we currently do not have information about the water quality.

In the revised manuscript, we added several new figures. Moreover, we believe we managed to improve significantly the self-consistency and the overall readability of the original plots.
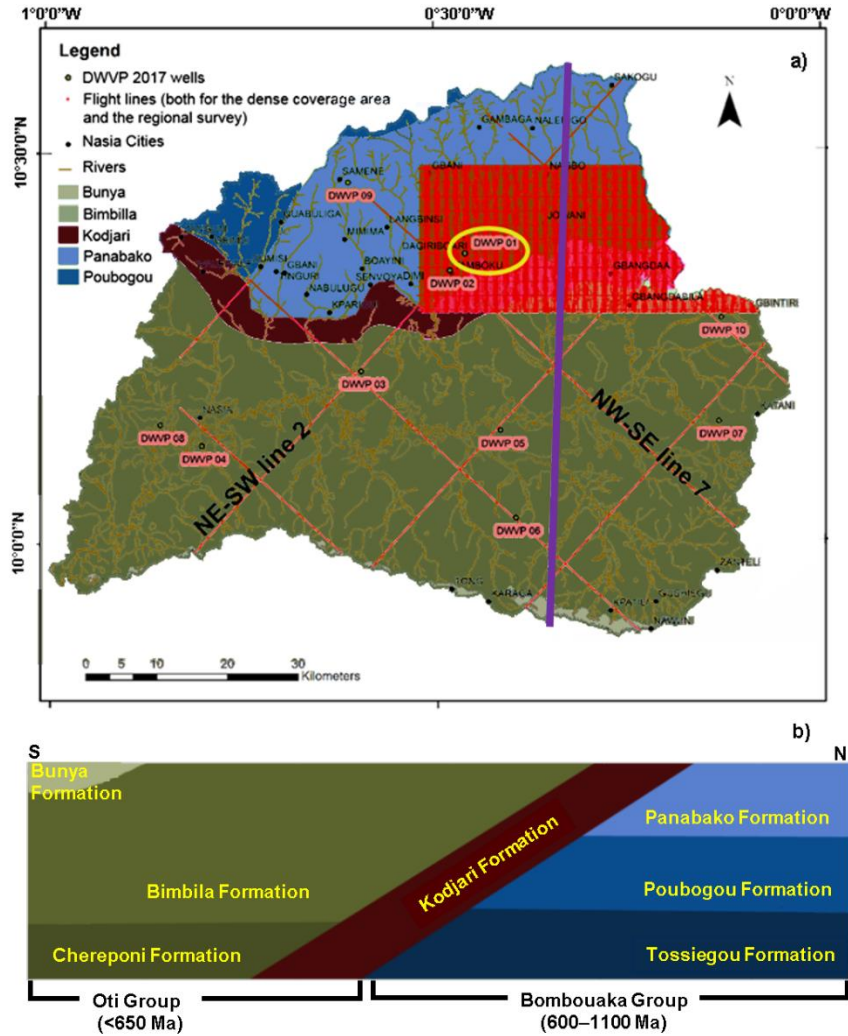
Figure R2.2: (a) Geologic Map of the Nasia sub-basin after Carney et. al (2010) [1]; the location of some of the available boreholes are indicated (e.g. DWVP01); the red solid lines represents the flight lines of the regional survey (20 km x 20 km grid) and of the dense coverage acquisition (200 m line spacing – in the NE of the Nasia basin – see, also, Fig. 9 in the revised manuscript). (b) Conceptual Model of the geology along a cross sectional N-S line within the study area - solid violet line in the panel (a).

With respect to the original Fig. 1, indications of the groups and their relationships with the formations have been made explicit. The age determinations for the Oti and Bombouaka are those in Kalsbeek et al. (2008) [2].

---

[1] Carney et al.: Lithostratigraphy, sedimentation and evolution of the Volta Basin in Ghana. Precambrian Research, 183, 701-724, doi:10.1016/j.precamres.2010.08.012, 2010.

[2] Kalsbeek et al.: Constraints on provenance, stratigraphic correlation and structural context of the Volta basin, Ghana, from detrital zircon geochronology: An Amazonian connection? Sedimentary Geology, 86-95, doi: 10.1016/j.sedgeo.2008.10.005, 2008.
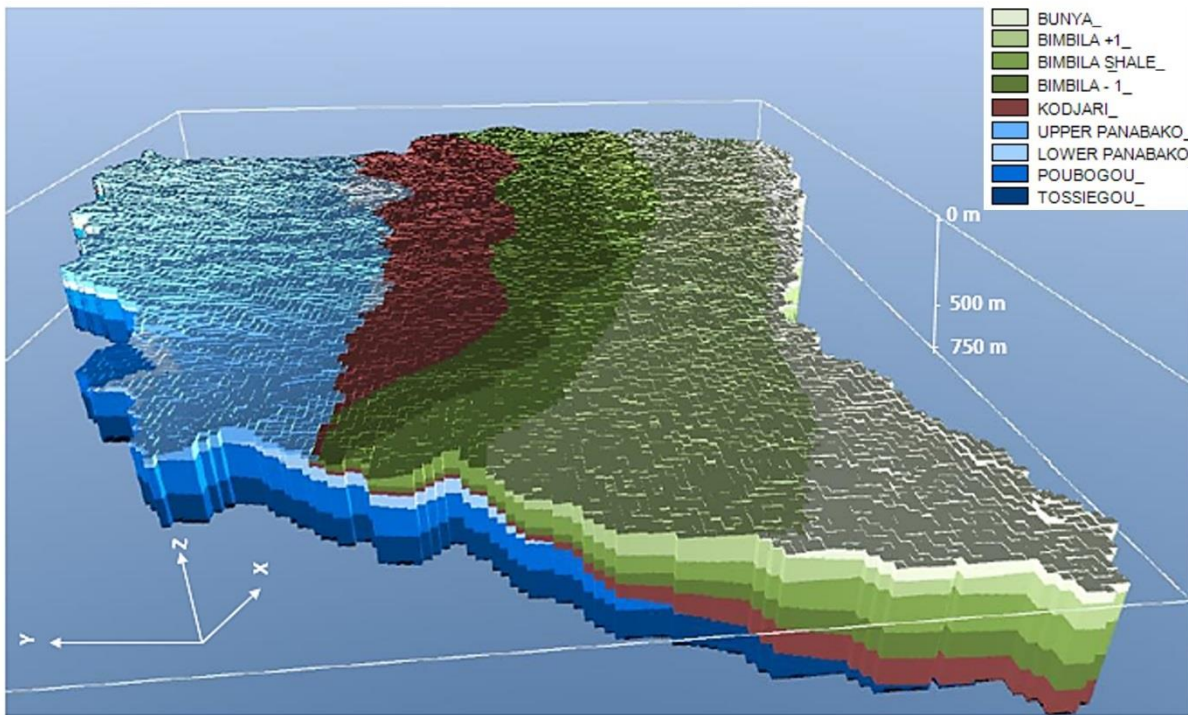
Figure R2.3: 3D geological model of the Nasia sub-basin resulting from the combined interpretation of the B-field airborne data, the prior geological knowledge of the area, and the available wells. With respect to the previous version of this figure, not only, now, the color scale is in agreement with the one of Fig. R2.2, but, in both of them, the legends follow the chronostratigraphic order (with the oldest located at the bottom).
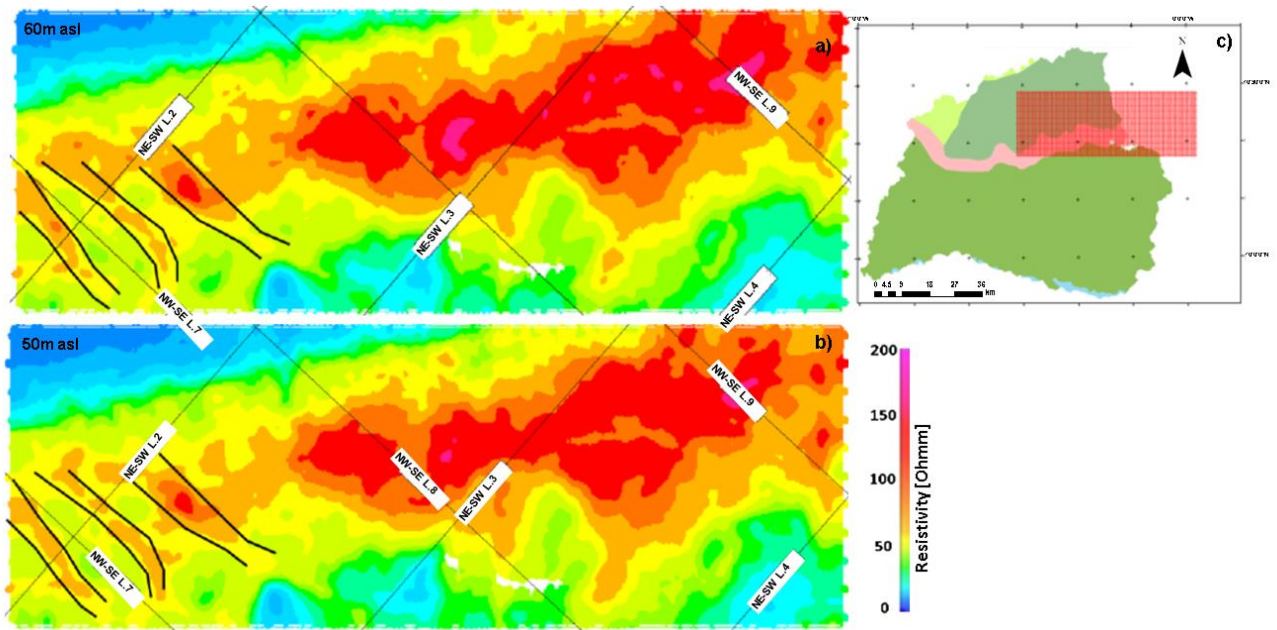
Figure R2.4: Horizontal resistivity slices at 60m (a) and 50 m (b) depth of the portion of the study area - in red in the panel (c) - characterized by a geophysical sampling much denser (200m line-spacing) than the regional survey - in this respect, see the lines from "NE-SW L.2" to "NW-SE L.9" in panel (a) and (b) characterized by a 20 km x 20 km spacing. The black solid lines in the left-bottom corner of panels (a) and (b) show the location of the paleovalleys discussed in the manuscript. Hence, the features interpreted as paleovalleys can be identified in both the two independently inverted datasets (i.e. the dense coverage area and the regional survey). Clearly, the densely sampled data can provide further insights in terms of spatial coherency of the paleovalleys' features.

New regional stratigraphic insights from a 3D geological model of the Nasia Sub-basin, Ghana, developed for hydrogeological purposes and based on reprocessed B-field data, originally collected for mineral exploration

Elikplim Abla Dzikunoo[1], Giulio Vignoli[2,3], Flemming Jørgensen[4], Sandow Mark Yidana[1] and Bruce Banoeng-Yakubo[1]

[1]Department of Earth Science, University of Ghana, Accra, Ghana

[2]DICAAR, University of Cagliari, Cagliari, Italy

[3]GRUK, Geological Survey of Denmark and Greenland (GEUS), Aarhus, Denmark

[4]Central Denmark Region, Viborg, Denmark

Correspondence to: Sandow Mark Yidana (yidanas117@gmail.com) and Elikplim Abla Dzikunoo (eadzikunoo@gmail.com)

Abstract. Re-processing of regional-scale airborne electromagnetic data is used in building a 3D geological model of the Nasia Sub-Basin, Northern Ghana. The resulting 3D geological model consistently integrates all the prior pieces of information brought by the electromagnetic data, lithologic logs, ground-based geophysical surveys and the geological knowledge of the terrain. The geo-modelling process is aimed at defining the lithostratigraphy of the area, chiefly to improve the stratigraphic definition of the area as well as for hydrogeological purposes. The airborne electromagnetic measurements, consisting of GEOTEM B-field data, were originally collected for mineral exploration purposes. Thus, those B-field data had to be (re)processed and properly inverted as the original survey and data handling were designed for the detection of potential mineral targets and not for detailed geological mapping. These new geophysical inversion results, compared with the original Conductivity Depth Images, provided a significantly different picture of the subsurface. The new geophysical model led to new interpretations of the geological settings and to the construction of a comprehensive 3D geomodel of the basin. In this respect, the evidence of a hitherto unexposed system of paleovalleys could be inferred from the airborne data. The stratigraphic position of these paleovalleys suggests a distinctly different glaciation history from the known Marinoan events, commonly associated with the Kodjari formation of the Voltaian sedimentary basin. Indeed, the presence of the paleovalleys within the Panabako may be correlated to mountain glaciation within the Sturtian age though no unequivocal glaciogenic strata have yet been identified. Pre-Marinoan glaciation is recorded in rocks of the Wassangara group of the Taoudéni basin. The combination of the Marinoan and, possibly, Sturtian glaciation episodes, both of the Cryogenian period, can be an indication of a Neoproterozoic Snowball Earth. Hence, the occurrence of those geological features, do not only have an important socio-economic consequences - as the

paleovalleys can act as reservoirs for groundwater - but, also from a scientific point of view, could be extremely relevant - as their presence would require a revision of the present stratigraphy of the area.

1 INTRODUCTION

35 The present research demonstrates the effectiveness of reprocessing and proper inversion of existing airborne electromagnetic (AEM) data - more specifically, GEOTEM B-field measurements - for data-driven inference of the subsurface geology. More specifically, the AEM results are employed to develop a 3D geological model for subsequent hydrogeological conceptualization, and scenario simulations of groundwater recharge and abstraction (under different environmental and anthropic stresses) in the partially metamorphosed sedimentary Nasia basinsub catchment (a sub-

40 catchment within of the White Volta Basin in Northern Ghana). In fact, the overall objective of the research is to develop a decision-support tool for understanding groundwater occurrence to facilitate efficient development and optimization of the water resources in the basin within the framework of the GhanAqua project (funded by DANIDA). The geological interpretation of the newly reprocessed AEM data has highlighted potential evidences of paleovalleys, which, in turn, might have great socio-economic and scientific impacts. Indeed, such geological features could be possible groundwater reservoirs

45 and lead to the revision of the current stratigraphy of the area.

The use of groundwater resources for crop irrigation offers an opportunity for a buffer against the unremitting impacts of climate change in Northern Ghana, where peasant farming is the mainstay of livelihood. The development of groundwater resources to support irrigation endeavours is particularly important because of erratic rainfall patterns during the rainy season and high temperatures and evapotranspiration rates in the dry season, which render surface water resources unsustainable

50 reservoirs of irrigation water (Eguavoen, 2008). Erratic rainfall patterns in the region in recent times have affected crop production and sustainable livelihoods of communities. Hence, improved access to groundwater resources for all year-round irrigation would boost agricultural development and offer increased employment possibilities in the area. However, over the years, access to sustainable groundwater resources has been hampered by the lack of sufficient knowledge of the local geological and structural geological setting. Such knowledge is crucial to the understanding of the hydrogeology and

55 groundwater storage conditions and would be crucial for sustainable resource development.

Generally, the difficulty in defining and effectively characterizing subsurface geological conditions in an area such as the Voltaian sedimentary basin hinges on the unavailability of enough reliable data (e.g., lithological logs of deep boreholes) and the limitations inherent in conventional ground-based geophysical techniques (e.g., poor spatial coverage and insufficient density). So, a multi-scale, holistic approach, integrating the airborne geophysical insights with all the available lithological

60 borehole logs and, former and present, ground-based geological investigations is showed shown to be essential for the development of an effective and coherent geological model to be eventually used for hydrogeological scenario assessments.

Three-dimensional (3D) geological modelling based on specifically collected AEM data for hydrogeological applications is, in general, not new (Jørgensen, Møller, et al. 2013; Jørgensen, et al. 2015; Høyer, et al. 2015; Oldenborger, et al., 2014), but

as far as we are concerned, it has never been done before using B-field measurements. Additionally, geological modelling for hydrogeological application is novel in the West African sub-region, even though the region has a rich database of pre-existing AEM data from former mineral exploration surveys. Hence, the application of the presented workflow for inversion of AEM data can potentially be extended to many areas in this part of the African continent, and, in general, everywhere pre-existing AEM data is available. This can help avoid the costs connected with the airborne data collection: which is often considered affordable for mineral exploration, but prohibitive for groundwater mapping.

~~In addition, the geological interpretation of the newly reprocessed AEM data (with their significantly enhanced information content) facilitated the discovery of evidence showing the presence of potential paleovalleys, possibly acting as groundwater reservoirs. At the same time, the existence of such geological features and, in particular, their stratigraphic location within the Panabako formation suggests the need for a possible revision of the stratigraphy of the Bombouaka group, especially within the study area. Additionally, the new insights suggest that there was some pre-Marinoan glacial activity responsible for the paleovalleys within the Panabako (Hoffman and Li, 2009) in the Voltaian sedimentary; preceding the Marinoan glaciation episode generally associated with the Kodjari formation of the basin (Deynoux et al. 2006) — both within the Cryogenian period. This new glaciation suggests that the possibility of a Sturtian event, but this assertion is currently hypothetical and would need further investigations to verify. The proposed combination of the Marinoan and Sturtian events in the Neoproterozoic Voltaian sedimentary basin, if verified would be compatible with the hypothesis of a global Neoproterozoic Snowball Earth even in low-latitude areas (Bechstädt et al., 2018; Hoffman and Schrag 2002).~~

Besides the (re)use of the above mentioned geophysical datasets, and in an attempt to address the main socio-economic issues connected with an effective hydrogeological characterization of the Nasia basin, the present research brings some contributions to the geological and stratigraphic knowledge of the Volta basin. Though the lithostratigraphy of the sedimentary infill of the Volta basin is still disputed (Blay, 1983; Affaton, 1990; Carney et al., 2008, 2010), there is a large consensus on its subdivision into three groups (Affaton, 1990; Affaton et al., 1980, 1991; Bertrand-Sarfati et al., 1991): Bombouaka, Oti (or Pendjari), and Obosum. In this research, we provide possible insights on the delineation of the interfaces between the formations characterizing the Nasia portion of the Volta basin; i.e. Bombouaka and Oti.

2 DATA AND METHODS

2.1 The Study Area

The approximately 5,300 km^2 area of the Nasia Basin is found in the ~~Northern~~ northern ~~Region~~ region of Ghana, within the Guinea Savannah belt. It is associated with an average annual rainfall of 1000-1300 mm, which peaks between late August and early September. Torrential rains within this peak season create serious drainage problems as the infiltration rates are low due to the largely impervious nature of the various lithologies, creating high amounts of runoff, in turn, leading to high levels of erosion and posing significant constraints on agriculture (FAO, n.d.).

95 The area is characterized by relatively low relief in the south, and a few areas of high elevation associated with the Gambaga escarpment to the north. The basin drains a left bank tributary of the White Volta, the Nasia River (Fig. 1a) and is underlain by sedimentary rocks of the Bombouaka and Oti-Pendjari groups of the Neoproterozoic Voltaian sSupergroup, and comprised predominantly of variations of sandstones, siltstones and mudstones (Carney et al., 2010). Detailed descriptions of the geologic units can be found in Carney et al., (2010) and, also in Jordan et al. (2009).

2.2 Data and Modelling Requirements

100 A 3D geomodel of an area is a synthesis of all relevant geologic information available; during the construction process, it is essential to integrate and merge multiple data sources and scales in order to appropriately represent the different aspects of a complex geologic systems (e.g., Dzikunoo et al. 2018; Rapiti et al, 2018; Jørgensen et al., 2015; Vignoli et al., 2017; Høyer et al. 2017; Vignoli et al, 2012). In this regard, the diverse kinds of data used in this study consist of: i) AEM data (namely,
105 GEOTEM B-field), ii) borehole lithological and geophysical logs, and iii) ground based Electrical Resistivity Tomography preexisting outcrop analyses and geological information(ERT).

An important underlying consideration for the construction of a lithostratigraphic model is the definition of a conceptual model initially developed from the prior knowledge of the terrain (Fig. 1b). Interpretations from geophysical signatures are then tied into the conceptual model followed by the development of a model framework with interpretation points and,
110 subsequently, populated with voxels, each characterized by homogeneous attributes. Clearly, any piece of information brought, in this specific case, from the geophysics can/must be used, via a confirmation/rejection process, to refine the initial geological hypotheses (Tarantola, 2006).

2.2.1 Airborne Electromagnetic Data (AEM)

A fixed-wing Casa 212 aircraft, equipped with a 20-channel GEOTEM multi-coil system, was used to acquire the time-
115 domain electromagnetic data (Fugro Airborne Surveys, 2009a,b) with both a line spacing of 20 km (flown at 042° - 132° along and across the general geologic strike lines within the Volta Basin) and a much denser line spacing of 200 m (flown at 000° - 180°). The locations of the flight lines of both surveys (dense and regional) are shown as red lines in Fig. 1a (the 200 m spacing makes the dense survey appear almost as a red rectangle). The GEOTEM surveys were performed under the auspices of the European Union Mining Sector Support Programme 2005 to 2008 and were designed for mineral exploration.
120 Within the present study, the original B-field data have been reprocessed and inverted; this is to ensure the preservation of all the corrections applied to the raw data by Fugro, and, contextually, to have the opportunity to consistently compare the new outcomes with the Conductivity Depth Images (CDIs) provided by the survey company as final deliverables (Fugro Airborne Surveys, 2009a,b). This comparison was necessary in order to estimate what could be gained by going through a complete reprocessing and inversion round in terms of reliability and accuracy of the subsequent (hydro)-geological model(s). Since
125 the data acquisition was originally focused on mineral targeting, the specifications of the survey, and, also, the choice of CDIs as deliverables, were intended to optimize the detection, even at depth, of large conductivity contrast targets (typical

for mineral exploration) with, potentially, a high lateral resolution. Conversely, for geological mapping purposes, the capability to retrieve, via proper inversion strategies, even low-contrast conductivity features and, at the same time, to reproduce the spatial coherence of the geological features is crucial. Therefore, it was important to double-check the effectiveness of the new inversion approaches and of the dedicated preliminary data conditioning.

In addition, to the advantages~~as~~ discussed in Smith and Annan, 1998, the choice of B-field has some further ~~advantages~~ benefits in terms of noise-signal ratio as the B-field is associated with data integration over time that can act as some sort of stacking in time. Clearly, the data stacking can (should) be performed also in the other "direction", that is, spatially, along the line of flight. ~~In the workflow implemented in this research, the optimal lateral time-dependent stacking window was selected by checking gate by gate the minimum width capable of preserving the spatial variability visible in the data, but, also, of reducing erratic oscillation of the signal.~~ In the workflow implemented in this research, a moving window with a width variable depending on the considered time-gate has been used in a fashion similar to the one detailed, for example, in Auken et al. 2009 and Vignoli et al. 2015 (but, here, the stacking window width is frequency-dependent). This strategy allows the use of: (i) a narrower time window at the early gates and (ii) a wider window at late gates where the signal has, in any case, a larger spatial footprint. By doing so, we can obtain the maximum spatial resolution at the near surface (where the signal is stronger) and, contextually, improve as much as possible the signal-to-noise ratio at depth (where, anyway, it is the physics of the method that is naturally averaging the information). In particular, the size of the window utilized for the Z-component of the B-field is linearly increasing from 7.911 s, for the first gate (4.505 ms), to 19.876 s, for the 11th gate (11.563 ms), and remains equal to 20 s for the last four gates; concerning the X-component, only twelve gates have been used, but with the same stacking window settings. An example of the data resulting from the application of this moving window strategy is shown in Fig. 2. In practice, these specific settings for the moving window have been selected through a visual trial-and-adjustment procedure aiming at removing the suspicious oscillations of the signal without laterally smoothing too much the data.

With respect to the inversion ~~,~~ as the receiver of the GEOTEM system is located in a towed-bird ~~,~~ altitude, pitch and roll of the device were part of the inversion parameters, and they were reconstructed by using the Z and X components of the B-field measurements and by enforcing a lateral continuity between ~~adjacent~~ nearby measurement locations. Similar approach has been used also for the main model parameter we inverted for~~:~~ the electrical resistivity. On the other hand, the thicknesses of the 30-layer parameterization have been kept fixed and have not been involved in the inversion. So, in the framework of a pseudo-3D inversion based on a 1D forward modelling, the resistivity of a specific discretizing layer was coupled to the resistivity values at the corresponding depths in the ~~closest~~ adjacent 1D soundings. Thus, for the data collected with a 200 m line spacing, we applied the so called Spatially Constrained Inversion (SCI – Viezzoli et al, 2008), while for the less dense acquisition data (20 km line spacing), its 2D version (Laterally Constrained Inversion - LCI) was used instead. The final results clearly depended on the specific choices of the inversion settings (e.g. the relative weight of the regularizing term connecting the resistivities of layers of different soundings) and the choices of the inversion strategy (e.g. sharp versus smooth regularization – Auken et al., 2014; Ley-Cooper et al. 2014; Vignoli et al., 2015; Vignoli et al., 2017). In order to

select the most effective regularization capable of retrieving a resistivity distribution compatible with: i) the observations within the noise level, and ii) the most reasonable geological expectation, we adopted an iterative geophysics-geology approach, characterized by a close interaction between geologists and geophysicist (Fig. 3). The basic rationale being~~behind this is~~ that the geological interpretation already starts at the geophysical processing stages. It is probably worth reminding, one more time, that the inversion of B-field curves (inevitably characterized by a finite number of gates and some level of noise) is an ill-posed problem (Tikhonov & Arsenin, 1977); thus, there are multiple solutions compatible with the data and those solutions may not be continuous with respect to data variations (so, small perturbations in the data may cause large differences in the final solutions, preventing self-consistent outcomes). Actually, regularization is about introducing in the inversion process the prior information about the kind of solutions we expect. Hence regularization selects, amongst all the possible solutions compatible with the data, the unique one that is also in agreement with our expectations (Zhdanov, 2015; Zhdanov, 2006). So, in inverting our datasets, we tested different kinds of regularizations; e.g. smooth, sharp, spatially constrained, laterally constrained, and, each of them, with different settings. Strictly speaking, since those diverse results were fitting the data at the same level, they were equally good from a purely geophysical perspective; thus, the intervention of the geologists, with their overall understanding of the possible geological structures and expectations was crucial. From an epistemological perspective, we can say that, to some extent, the geophysics has been used to falsify some of the geological alternatives - i.e. those that were not fitting also the geophysical data (Tarantola, 2006). The models in agreement with both the geophysical data and the geological expectation have been used to (qualitatively) asses the uncertainty of the geophysical models (Fig. 3). In this respect, stochastic inversion would have been the optimal solution to explore (quantitatively) the ambiguities of the geophysical solutions; unfortunately, stochastic inversion schemes are still not available (or, at least, not practically feasible) for problems at this scale. On top of this, propagating the uncertainty of the geophysical solutions into the uncertainty of the geomodel is still an open (and extremely relevant) question.

For the large majority of the Nasia sub-catchment, a smooth regularization has been used with extremely loose (compared with those generally used for the standard dB/dt-data inversion – e.g., Viezzoli et al. 2010 and Viezzoli et al. 2013) lateral and vertical constraints. The result is a quasi-3D resistivity volume generated from B-field GEOTEM data that is significantly different (in terms of possible geological interpretation) from the original CDIs (Fig. 4).

~~2.2.2 Electrical Resistivity Tomography~~

~~2D ERT surveys were performed at different locations in order to optimally site new boreholes and to investigate the nature of the near subsurface within the study area. Figure 1a shows the locations of the DWVP wells which were sited using ERT. ERT lines were extended to either 400 m or 800 m with electrode spacing of 20 m.~~

~~The observed apparent resistivities have been processed to remove evident spurious data points, and, subsequently, inverted using RES2DINV (Meier, et al., 2014; Loke, 1997; Loke and Barker, 1996) (Fig. 3).~~

2.3 3D Geo-modelling Procedure

2.3.1 Bedrock Geology

Raw data collected from various sources can be interpreted in terms of spatial variations (providing information about the geometries) and/or in terms of the absolute value of the attribute retrieved from the data (characterizing, not only the geometry of the features, but also their nature).

The spatial information from the geophysics was used to create a 3D geometry model. Geometric modelling involves two steps. The first concerns the development of a suitable geometric representation of the fundamental geological "framework"; the second relates to the discretization of this framework to provide control for the analytical computations within the numerical models used in the predictive modelling (Turner, 2006).

In the present research, the first stage in the geometric modelling involved the interpolation of inverted 1D AEM data (Fig. 5) into a 3D grid with an assigned search radius of 20 km and a cell size of 2 km, for the regional data, and a search radius of 500 m and a cell size of 100 m, for the dense area. The assigned search radius should be not be less than the spacing between flight lines, to obtain continuous electrical resistivity distribution (Pryet et al., 2011), but, at the same time, it needs to be small enough to prevent smearing of possible useful information. The second, more laborious, step involved constructing the surfaces which define the overall units. Here, both the AEM and borehole data were correlated to a particular stratigraphic unit and the boundaries for that unit were drawn. This is necessary, and very tricky, since the electrical resistivity as it is inferred from the AEM cannot be unambiguously made to correspond to a specific lithology/stratigraphic unit. Clearly, for this task, not only the knowledge of the geophysical response behaviour, but, clearly, also the experience of the geologists in outlining which signatures belong to which stratigraphic unit, are equally crucial. For instance, low resistivity signatures within the Bombouaka may belong to the Poubogou formation, whereas anomalies with similar low resistivity ranges within the Oti may belong to the Bimbila formation. Also for this reason, the tight interaction between geologists and geophysicists (through several iterations) has been found crucial for an effective geomodelling - for example, in interpreting the geological features where the geophysical reliability is reducing as we get closer to the Depth of Investigation (DOI – the shaded portion at the bottom of Fig. 4b).

Thus, the geomodelling can be considered as a way to compile, in a consistent manner, the geological knowledge about the area, the information from the dense geophysics (which acts as a "smart" interpolator between the available boreholes) and the other ancillary available data. In this respect, it is worthwhile to note that only boreholes which had a distance smaller than 1-3 km from the regional flight lines were considered sufficiently representative for the geophysical interpretation.

The outlined boundaries were, then, used, in the next stage, for populating the model grid (Ross et al., 2005; Sapia, et al., 2015; Jørgensen, et al., 2013). Populating the model grid is done by adding and editing voxel groups based on a cognitive approach (Fig. 6 - Høyer, et al., 2017; Høyer, et al., 2015; Jørgensen, et al., 2013).

2.3.2 Regolith

The AEM data does not have the sufficient shallow resolution to effectively investigate the regolith layers that, however, are fundamental to understand the shallow groundwater behaviour. It is also for this reason that ERT data were collected and used to infer the weathered zone. The regolith depths were derived from borehole logs and ERT interpretations, and gridded to form a basal surface, referred to as the bedrock surface in Gulbrandsen et al. (2018). Depth ranges of between 2 – 42 m were obtained. There was no significant difference in the regolith thicknesses across the Bombouaka and Oti groups within the study area. The depth to regolith estimates were used by the hydrogeologists in setting constraints for a hydrogeological model which defined recharge and flow within the basin. Outlines of the regolith, as they can be found in Geological Survey Department (2006), were used as constraints, together with the terrain and the regolith depth grids, to create the 3D interpolation (Fig. 6a).

The obtained 3D regolith grid was then merged with the 3D bedrock grid to offer a complete picture of the subsurface geology (Fig. 6b).

3 RESULTS AND DISCUSSIONS

3.1 Inverted AEM data

Figure 4 shows an example of the comparisons between the original CDIs and the new inversion obtained with the discussed smooth SCI approach applied on the B-field GEOTEM data. The differences are evident. Not surprisingly, the CDI result is characterized by higher lateral variability, as each sounding is converted into a resistivity profile independently, while the SCI, by definition, enforces some degree of spatial coherence. The more prominent CDI's lateral heterogeneity is clear not only, on the N-E side of Fig. 4a, in the shallow portion of the section, where well distinct resistive inclusions are detected, but also, at depth, along all the flight lines where there are spurious lateral oscillations of the electrical properties. The SCI result is laterally more consistent; however this does not prevent the reconstruction of a resistive body (associated with the hotter colours), at a distance of approximately 10 km (circled in red - Fig. 4b), that is well-separated from the resistive superficial unit - continuing on the right - by a clear conductive formation (very differently from what is retrieved by the CDI). In addition, the SCI result shows interesting resistive features incised into the more conductive surroundings (in particular, cfr. the two deepening structures located between 20 and 30 km – circled in black in Fig. 4b). It is worth noting the considerable depth of investigation (DOI - indicated as a white mask in Fig. 4b); generally, the geophysical model parameters can be considered sensitive to the data down to the considerable depth of ~500 m. This, not only, demonstrates the quality of the original data, but, also, confirms that the survey was designed for deep exploration and not for high-resolution shallow investigations. Therefore, the new SCI provides important insights on the geological settings and highlights resistive, relatively shallow structures, possibly relevant as groundwater reservoirs.

In order to proceed further with the geological interpretation of the geophysical model, the SCI result was gridded (Fig. 5). The general signature trends visible in such a resistivity grid can be summarized as follows:

255 •   areas with low resistivity values characterize argillaceous layers; in both the Bombouaka and Oti ~~groups;~~

•   sandstones have characteristically high resistivity values, with the massive quartzose sandstones of the Bombouaka ~~and Kwaku g~~Groups (specifically, the Panabako ~~s~~Sandstone, Anyaboni ~~s~~Sandstone,~~–~~ and ~~upper~~ Upper Damongo ~~Formation~~formation) displaying the lowest conductivities (Fugro Airborne Surveys Interpretation, 2009b).

260 **~~3.2 Inverted ERT data~~**

~~The difference in resistivities between fresh rocks and their weathered equivalents enable demarcation of the weathered zone. The example in Fig. 3 demonstrates the capability of electrical resistivity to outline the weathered zones. These geophysical observations are then compared against the available borehole data. Along this profile, three distinct layers are observed: i) the first one has high resistivities towards the southwest and decreasing values towards the northeast; ii) the~~

265 ~~second layer has low to moderate resistivities; and iii) the deepest is characterized again by high resistivities.~~
~~Considering the terrain, i.e. Panabako sandstones within which this profile was undertaken (Fig. 1a), it can be inferred that:~~

~~i)   The first layer towards the southwest, which is approximately 10 m thick, with an average resistivity of 500 to more than 5000 Ohm-m, is the weathered zone which includes hardpan alternatively referred to as the saprolite and saprock. From the midpoint, towards the NE, resistivity signatures are similar to that of the underlying~~

270 ~~second layer.~~

~~ii)   The second layer, which is approximately 30 m thick, can be considered to be part of the bedrock. Its characteristic low resistivity signature could be attributed to a fracture system (at the midpoint of the profile), confirmed by the evidences observed during drilling between the depths of 40 m to 50 m below the surface; the sandstones records resistivity values between 22 to 490 Ohm-m. Additionally, the profile is less than 5 km~~

275 ~~away (at both ends of the line) from regional E-W (sensu lato) brittle faults identified by Crowe & Jackson-Hicks (2008).~~

~~iii)   The bedrock, which is made up of fresh feldspathic quartz rich arenites, records resistivity values between 500 and >5000 Ohm-m.~~

Figure 6 shows the 3D geological model of the study area. ~~They~~ It ~~are~~ is mainly based on the geophysics ~~(ERT, AEM)~~ and

280 the ~~ancillary~~ other source of available information (regolith outlines from previous radiometric survey - Geological Survey Department, 2006). The developed ~~Nasia Basin~~ geological model ~~(Fig. 6) consists of 17.5 million voxels, each with 500 m x 500 m lateral size and 5 m thickness. The model~~ (consisting of 17.5 million 500 m x 500 m x 5 m voxels) shows a coherent 3D representation of the subsurface within the Nasia Basin ~~including the weathered zone.~~; ~~This~~ it generally honours the available geologic knowledge as well as the information from the wells, and the AEM evidences. ~~Moreover~~At the same time,

285 it provides some new insights into the geology of the terrain.

3.3 Lithostratigraphy from AEM

Figure 6 shows nine distinct stratigraphic units in the study area. These include: i) Bunya (Youngest), ii) Bimbila +1, iii) Bimbila Shale, iv) Bimbila -1, v) Kodjari fFormation, vi) Upper Panabako sSandstone, vii) Lower Panabako sSandstone, viii) Poubogou fFormation and ix) Tossiegou ~~Formation~~ formation (Oldest).

3.3.1 The Bombouaka Group

In the study area, the Poubogou and Panabako formations of the Bombouaka gGroup outcrop in the north. On the contrary, outcrops of the basal unit of this group, the Tossiegou Formation, have not been observed within the study area.

Tossiegou Formation

This is the oldest unit of the Bombouaka group identified by resistivity signatures ranging approximately between 30 and 120 Ohm·m. on cross sections of the inverted AEM volume. ~~This is the oldest unit of the Bombouaka group. Rocks of this formation are not seen outcropping in the study area. However, their signature is picked from the inverted AEM data as ranging approximately between 30 and 120 Ohm·m.~~ The formation is comprised of basal argillaceous strata which grade upwards into feldspathic and quartzitic sandstones (Carney, et al., 2010). They overlie crystalline basement rocks of the Birimian (Anani et al., 2017). For example, from the NE-SW section across the resistivity volume shown in Fig. 7, the Tossiegou formation is seen to extend way beyond 140 m below sea level. An estimation of the thickness of the formation is, however, made difficult by its extension below the DOI. In fact, the great depth of the formation, together with the overlying more ~~–~~ conductive layers (the Bimbila and Poubogou formations), generally, prevent the electromagnetic signal from propagating to greater depths making the inferred resistivity values of that formation poorly sensitive to the data (and so, difficult to be resolved precisely).

Poubogou Formation

This unit is identified within ~~confined to~~ the Gambaga escarpment with an average thickness of 170 m ~~and grades upwards into the Panabako formation with an increase in the arenaceous material~~ (Fig. 7). The basin-wide distribution of this sequence indicates a possible regional transgression event (Fugro Airborne Surveys Limited, 2009). The formation consists of green-grey, micaceous mudstones and siltstones intercalated with sandstones at some places. As it grades into the overlying Panabako formation, there is an increase in the sandstone proportion relative to the argillaceous beds (Carney et al., 2010). This formation exhibits low ~~poor~~ resistivity in AEM profiles ranging between 0 to 20 Ohm·m and appears to have a ~~thicknesses~~ thickness in the range of 150-180 m along a NE – SW profile in the study area. This is consistent with thicknesses recorded by Carney et. al (2010).

Panabako Formation

This is a quartz-arenite rich formation with a suggested thickness of 150-200 m (Carney et al., 2010). Lithostratigraphic
mapping by Ayite et al. (2008) identified two subdivisions of the Panabako Formation within the Nakpanduri escarpment.
The upper division consists of near shore aeolean sequence, while the lower sequence is composed of near shore fluvial
sequence (~~lower~~ Lower Nakpanduri ~~s~~Sandstone formation); Carney et al. (2010) correlate the ~~lower~~ Lower Nakpanduri to
~~upper~~ Upper Poubogou. From the current AEM data, this subdivision is however observed entirely within the Panabako with
the presence of a distinct resistivity contrast clearly visible in the newly inverted data (e.g. Fig. 7); indeed, in the new AEM
reconstruction, the upper Panabako shows higher resistivities - ranging from approximately 60 to 200 Ohm·m - and the
lower layer is characterized by relatively moderate conductivity - roughly between 30 and 60 Ohm·m. The tendency of the
Bombouaka ~~g~~Group ~~sandstone~~ sandstone units to fine towards argillaceous strata at their base (Jordan et al., 2009) can be
inferred from the increasing conductivity values towards the base, indicating a probable increase in argillaceous material.

3.3.2 The Oti Group

This group underlies the southern portion of the study area. Generally, it records the transition from a shallow marine
environment adjacent to a rifted margin into a marine foreland basin sequence represented by interbedded argillaceous and
immature arenaceous material (Carney et al., 2010).

Kodjari Formation

Composed of what is commonly known as the triad, this formation constitutes the basal unit of the Oti Group (Fig. 6).
Commonly, the Kodjari formation comprises: (i) basal tillites followed by, (ii) a cap-carbonate limestone, and finally
covered with (iii) laminated tuffs and ash rich siltstones (Carney et al., 2010).
The presence of the Kodjari formation is not easily ~~seen, but~~seen but can be inferred from the SCI resistivity sections by
moderately resistive strata observed immediately above the topmost units of the Bombouaka group (Fig. 7). An average
thickness of 75 m can be retrieved; however, it should be noted that its continuity throughout the basin has not been verified.
Carney et al., (2010) noted that, at some localities, in the north of the Volta Basin, the overlying tuffaceous material of the
Kodjari triad is seen to unconformably lie directly on the Panabako rocks of the Bombouaka as a result of the lateral
discontinuity of these units. These occurrences are confirmed also in the reprocessed AEM data (e.g. Fig. 7, at around ~~110~~40
- ~~120~~45 km).

Bimbila Formation

The Bimbila formation has two sandstone beds forming its upper and lower boundaries. These are the Chereponi ~~s~~Sandstone
member which form~~s~~ the basal stratum of the formation and the Bunya ~~s~~Sandstone member, which generates the exposed

upper portion of the formation. The Bunya sandstone is observed as a moderately conductive layer in the AEM cross section,

above the argillaceous material of the Bimbila (Fig. 7).

The argillaceous units of the formation consist mainly of green to khaki, micaceous laminated mudstones, siltstones and sandstones representing a continuation of foreland basin deposition.

3.4 Structural Interpretations

The new results from the inversion of the AEM data reveal some amount of deformation within the basin. ~~The arcuate nature of the basin, in addition to some other structures, is observed in the cross sections.~~ Dips of approximately 20° to the SW of the Bimbila are seen from AEM interpretations giving an indication of the arcuate nature of the basin.

~~Figures 7 and 8 show the generally curved nature of the basin with dipping (approximately 20° from the surface) side slopes within the Bimbila.~~

Along ~~line~~ NE-SW line 7 (Fig. 8), a vertical displacement is observed and is interpreted as a fault within the Bimbila. It aligns well (*sensu lato)* to late brittle faults (Crowe & Jackson-Hicks, 2008).

An angular unconformity marking the transition between rocks of the Bombouaka (which began, accordingly to Carney et al. (2010), to accumulate after 1000 Ma) and the Oti rocks (which have a maximum depositional age of 635 Ma – Carney et al., 2010) are observed in Fig. 7. The unconformity could possibly be related to the absence of zircons aged between 950 – 600 Ma recorded by Kalsbeek et al. (2008), suggesting the presence of an oceanic gap which prevented the deposition of sediments. The unconformity separates continental deposits of the Bombouaka below, from passive margin deposits of the Oti above (Kalsbeek et al., 2008).

~~An angular unconformity marking the transition between rocks of the >1000 Ma old Bombouaka rocks and the 700-600 Ma Oti rocks (Kalsbeek et al., 2008) are observed in Fig. 76. The unconformity and the absence of sediments aged between 600 – 950 Ma could suggest the presence of an oceanic gap which prevented the deposition of sediments (Kalsbeek et al., 2008). The unconformity separates continental deposits of the Bombouaka below, from passive margin deposits of the Oti above (Kalsbeek et al., 2008).~~

Paleovalleys

Three characteristic "U-shaped" valleys towards the north of the basin were interpreted from AEM data, between ~ 53 km and ~ 63 km, along the profile in Fig. 7 (highlighted by black arrows), being resistive features at the base of the Upper Panabako, cutting into the Lower Panabako. The valleys exhibited a NW-SE trend (Fig. 9) and are considered to be tunnel valleys (Jørgensen & Sandersen, 2006; Kehew et al., 2012; Van der Vegt et al., 2012) whose origin is still to be fully investigated. The presence of these valleys may be of stratigraphic interest as well as hydrogeologic significance.

~~Characteristic "U - shaped" valleys were interpreted from AEM data to the north of the basin (Fig. 7). The valleys exhibited a NW-SE trend and are considered to be tunnel valleys (Jørgensen & Sandersen, 2006; Kehew et al., 2012; Van der Vegt et~~

al., 2012), the origin of which is still to be investigated. However, the presence of these valleys may be of stratigraphic interest as well as hydrogeologic significance.

390 The proposed presence of valleys between the Upper and Lower Panabako sequences represents an unconformity before the deposition of the Upper Panabako sequence (Fig. 7). The geometry of the valleys, with their ~~deep 'U'~~-shaped cross sectional nature, leads to the deduction that glaciation could play a role in their formation. Moreover, new insights into the stratigraphy may be implied with the possible presence of these valleys within the Panabako formation. The high energy event responsible for producing the intra-formational unconformity, most likely, occurred within the wide age range of

395 ~1000 Ma to 635 Ma (Carney et al. 2010). The upper limit defined by the detrital zircon analysis of the Bombouaka group (Kalsbeek et al., 2008). Whereas, the lower limits, representing the period of deposition of the tillites and diamictons of the Oti group within the Kodjari formation, should ~~coorrespond~~correspond to the end of the Cryogenian glacial period, which has been dated at 635 Ma by ~~(~~Carney, et al., 2010~~)~~. This possible event would, however, be younger than the 1100 Ma deposition of sediments of the Bombouaka based on detrital zircon analysis as discussed in Kalsbeek et al. (2008). These

400 valleys, then, represent a distinct history of glaciation separate from the Marinoan glaciation recorded in the Kodjari (Porter et al., 2004). This is similar to what is seen in the Wassangara group (Deynoux et al., 2006; Shields-Zhou et al., 2011) of the ~~Taoudeni~~Taoudéni basin outcropping in western Mali and southern Mauritania. Located in the southern region of the ~~Taoudeni~~Taoudéni basin, thick successions of glacial influence have been recorded (Shields-Zhou et al., 2011) and were initially thought to form a part of Supergroup 2 of the ~~Taoudeni~~Taoudéni basin. However, ~~their~~ the paleovalleys' presence

405 below the craton wide erosional and angular unconformity marking the transition between Supergroup 1 and 2 precludes their association with the Marinoan glaciation of Supergroup 2 and includes them in what is referred to as the Wassangara group rocks of Supergroup 1 (Deynoux, 2006; Shields-Zhou et al., 2011). Previous research within the Voltaian, are replete with information on the glaciation within the Neoproterozoic Marinoan where an unconformity between the top of the Bombouaka group and the basal units of the Oti-Pendjari group was proposed. This unconformity is conspicuously marked

410 by 'the Triad', consisting of basal tillites, cap carbonates and silicified tuffs (Goddéris et al., 2003).

On the other hand, Deynoux et al., (2006) mention that the 400-500 m thick glacially influenced succession was controlled by the tectonic evolution of the nearby Pan-African belt with deposition at around 660 Ma. These proposed pre-Marinoan, or possibly Sturtian (~717 to 643 Ma), glacial events and deposits are suggested to be related to mountain glaciers (Bechstädt et al. 2018; Deynoux et al. 2006; Hoffman and Li 2009; Villeneuve and Cornée 1994). Though these assertions are ~~largely~~

415 hypothetical, they ~~are feasible because of~~might be consistent with the ~~low~~ high-paleolatitude ~~position~~ of the West African craton during the Proterozoic (Bechstädt et al. 2018; Hoffman and Li 2009) combined with other geophysical and correlative evidence on the same craton (Dzikunoo et al., 2018; Shields-Zhou, et al. 2011) ~~evidence on the same craton~~.

The rocks of the Bombouaka group in the Voltaian sedimentary basin are said to be reminiscent of the rocks in portions of Supergroup 1 in the ~~Taoudeni~~Taoudéni basin (Shields-Zhou et al., 2011) and the presence of glacial signatures in both

420 groups suggests that the pre-Marinoan glaciation must have been regional. The trends of the paleovalleys in the study area, i.e. NW-SE (Fig. 9) align well to paleogeographic reconstructions of glaciation in the NW Africa region which suggest the

presence of an ice sheet towards the north of the Reguibat shield with inferred glacial movement southwards towards the Pan-African belt (Shields-Zhou et., 2011). The glacial movement is further verified by the transition of sediments in the region from glacial to a mixture of glacial and marine and finally marine towards the border with the rocks of the Pan

425 African belt. Some authors consider that the combination of Sturtian and Marinoan glaciations - both of the Cryogenian - suggest a complete glaciation event; i.e. the Snowball Earth where both continental and oceanic surfaces were covered by ice (Goddéris et al. 2003; Hoffman and Li 2009; Macgabhann 2005). A possible point of contention for the Snowball Earth hypothesis – that clearly suggests the ubiquitous presence of ice-sheets during the Marinoan and Sturtian (including the warmest parts proximal to the paleoequator, and, consistently, also, the higher paleolatitudes and high elevations) – is the

430 lack of such glacial evidences in the West Africa craton from the Sturtian. In fact, within the framework of that hypothesis, quite complex assumptions (Hoffman & Li, 2009) have been made in the attempt to justify the absence of glacial traces in the West Africa craton located, during the Sturtian, in cold regions (latitude around 60° S – Lie et al., 2008). So, the presence of the discussed glacial paleovalleys in the Voltanian can easily fill the gaps with no need of additional ad-hoc assumptions. On the other hand, t

435 The lack of pervasive evidences of the Sturtian glaciation within the Voltaian and the ~~Taoudeni~~Taoudéni could be due to the overprinting of glacial structures by the more recent Marinoan glaciation or tectonic activity related to regional subsidence during the evolution of the Voltaian (Ayite, ~~Awua, and Kalvig~~et al., 2008).

Outcrop investigations of samples from the Bombouaka, however, do not show mixtites/diamictites which are typical of glacial deposits and could either suggest a re-working of the glacial deposits by some fluvial action; this seems quite similar

440 to the situation Bechstädt et al. (2018) refers to as post-glacial transgression resulting in the infilling of incised valleys with fluvial, reworked glacial and marine deposits. Carney et al. (2010) observed two sandstone sequences in the Panabako with the upper unit forming 'sugarloaf' cappings above the lower sandstones. These structures are characteristic of high energy environments (Ayite et al., 2008) and may also be remnants of the Sturtian glaciation reworked by some marine or fluvial activities.

445 To summarize, the geological interpretation of the newly reprocessed AEM data (with their significantly enhanced information content) facilitated the discovery of evidence showing the presence of potential paleovalleys, possibly acting as groundwater reservoirs. At the same time, the existence of such geological features and, in particular, their stratigraphic location within the bounds of the Panabako formation suggests the need for a possible revision of the stratigraphy of the Bombouaka group, especially within the study area. Furthermore, the new insights suggest that there was some pre-

450 Marinoan glacial activity responsible for the paleovalleys within the Panabako (Hoffman and Li, 2009) in the Voltaian sedimentary basin; thus, this activity precedes the Marinoan glaciation episode - that is generally associated with the Kodjari formation of the basin (Deynoux et al. 2006) - but still occurs within the Cryogenian period. This new glaciation suggests the possibility of a Sturtian event, but this assertion is currently hypothetical and would need further investigations to verify. Possible glacial incisions within the Panabako seem reasonable because of high-paleolatitude of the West Africa craton, but,

455 at the same time, can avoid the need for additional complex justifications for the absence of indications of ice-sheets in

poleward continents. Hence, the proposed combination of the Marinoan and Sturtian events in the Neoproterozoic Voltaian sedimentary basin, if verified, would be compatible with the hypothesis of a global Neoproterozoic Snowball Earth even at high-paleolatitudes (Hoffman and Schrag 2002).

460 **3.5 Hydrogeological applications of the Geological Model**

The 3D geological model developed in this research is to be used as the basis for conceptualizing the hydrogeological context of the basin and the larger Voltaian sSupergroup. For instance, the apparent detection of the valleys within the Panabako formation may provide an indication of a deeper, prolific aquifer system which has not been noted before in the hydrogeology of the Voltaian sSupergroup. The presence of such systems in the Voltaian would have significant

465 implications for the large scale development of groundwater resources for irrigation and other income generation ventures in the area. The Voltaian sSupergroup has been noted as a difficult terrain in terms of groundwater resources development and the Nasia bBasin, in particular, is one of the basins where high borehole failure rates have led to chronic domestic water access challenges over several years. Within or after the current DANIDA project, the paleovalleys need to be further investigated, leading to both seismic investigations surveys and the drilling of much deeper boreholes penetrating them.

470

3.6 Conclusion

The present research investigates the concrete possibility of using pre-existing airborne electromagnetic data, originally collected for mineral exploration, to build accurate 3D geological models for hydrogeological purposes. The use of this specific kind of data (B-field time-domain electromagnetic measurements) for this scope is quite novel per se and, in this

475 specific case, allowed the reconstruction of the stratigraphy of the Nasia basin within the Voltaian sedimentary basin. In particular, the proposed geomodelling strategy made possible to infer the presence of paleovalleys paleochannels that have been identified as being pre-Marinoan and may be products of a glaciation event within the Sturtian (old-Cryogenian). The valleys correlate with glacial deposits observed in the Wassangara group of the TaoudeniTaoudéni basin. This group is found within the Supergroup 1, which correlates with the Bombouaka rocks of the Voltaian basin. If confirmed, the stratigraphic

480 location of these potential paleovalleys within the Panabako formation would lead to a possible revision of the stratigraphy of the Bombouaka group, especially within the study area. Moreover, Togethertogether, the paleovalleys and the glacial deposits give further evidence for a snowball earth event that possibly covered the entire Earth during the Neoproterozoic. So, the impact of these finding goes beyond the discovery of potential groundwater reservoirs (by itself-, extremely relevant from a socio-economic perspective) and can contribute to a rethinking of the stratigraphy of the region and confirm the

485 Neoproterozoic Snowball Earth hypothesis.

Author Contribution

490 **Elikplim Abla Dzikunoo**: Investigation, Data Curation, Methodology, Visualization, Writing – original draft, Writing – review & editing;

Giulio Vignoli: Conceptualization, Funding Acquisition, Investigation, Data Curation, Methodology, Software & Algorithm development, Supervision, Validation, Writing – review & editing;

Flemming Jørgensen: Investigation, Methodology, Supervision, Validation, Writing – review & editing;

495 **Sandow Mark Yidana**: Conceptualization, Funding Acquisition, Project Administration, Supervision, Validation, Writing – review & editing;

Bruce Banoeng-Yakubo: Supervision.

500 **Acknowledgments**

The authors would like to thank DANIDA for its support to this research through the South-driven project: "Ground Water Development and Sustainable Agriculture (Proj. Code: 14-P02-GHA)", also known as "GhanAqua"; and the Geological Survey Authority of Ghana for providing most of the data and for its invaluable help. In this respect, a special thank goes to Mr. Mensah and the director, Dr. Duodu. In addition, the authors are very grateful to Kurt Klitten and Per Kalvig from the

505 Geological Survey of Denmark and Greenland for their love for Ghana and for making this adventure possible.

References

Affaton, P., Sougy, J., & Trompette, R.: The tectono-stratigraphic relationships between the Upper Precambrian and Lower Paleozoic Volta Basin and the panAfrican Dahomeyide Orogenic Belt (West Africa). American Journal of Science, 280, 224–248, 1980.

510 Affaton, P.: Le Bassin des Volta (Afrique de l'Ouest): une marge passive, d'âge Protérozoïque supérieur, tectonisée au Panafricain (600 ± 50 Ma). Edition del'ORSTOM, Collection Etudes et Thèses, Paris, 2, 499, 1990.

Affaton, P., Rahaman, M.A., Trompette, R., & Sougy, J.: The Dahomeyide Orog: tectonothermal evolution and relationships with the Volta Basin. In: Dallmeyer, R.D., Lecorche, J.P. (Eds.), The West African Orogens and Circum-Atlantic Correlatives. Springer, New-York, 107–122, 1991.

515 Asch, T., Abraham, J., & Irons, T.: A Discussion on Depth of Investigation in Geophysics and AEM Inversion Results, SEG Technical Program Expanded Abstracts 2015, 2072-2076, https://doi.org/10.1190/segam2015-5915199.1, 2015.

Anani, C. Y., Mahamuda, A., Kwayisi, D., & Asiedu, D. K.: Provenance of sandstones from the Neoproterozoic Bombouaka Group of the Volta Basin, northeasten Ghana, Arab J Geosci., 10, 465, doi: 10.1007/s12517-017-3243-2, 2017.

Auken, E., Christiansen, A.V., Westergaard, J.H., Kirkegaard, C., Foged, N., & Viezzoli, A.: An integrated processing scheme for high-resolution airborne electromagnetic surveys, the SkyTEM system, Exploration Geophysics, 40, 184-192, 2009.

Auken, E., Christiansen, A. V., Kirkegaard, C., Fiandaca, G., Schamper, C., Behroozmand, A. A., Binley, A., Nielsen, E., Effersø, F., Christensen, N. B., Sørensen, K., Foged, N., & Vignoli, G.: An overview of a highly versatile forward and stable inverse algorithm for airborne, ground-based and borehole electromagnetic and electric data, Exploration Geophysics, 46, 223-235, doi:10.1071/EG13097, 2014.

Ayite, A., Awua, F., & Kalvig, P.: Lithostratigraphy of the Gambaga Massif, The Voltaian Basin, Ghana, Workshop and Excursion, March 10-17, 2008, 41-44, 2008.

Bechstädt, T., Jäger, H., Rittersbacher, A., Schweisfurth, B., Spence, G., Werner, G. & Boni, M.: The Cryogenian Ghaub Formation of Namibia–new insights into Neoproterozoic glaciations, Earth-science reviews, 177, doi: 10.1016/j.earscirev.2017.11.028, 678-714, 2018.

Bertrand-Sarfati, J., Moussine-Pouchkine, A., Affaton, P., Trompette, R., & Bellion, Y.: Cover sequences of the West African Craton. In: Dallmeyer, R.D., Lécorché, J.-P. (Eds.), The West African Orogens and Circum-Atlantic Correlatives. Springer-Verlag, Berlin, pp. 65–82, 1991.

Bernard, J.: Short note on the depth of investigation of electrical methods. Orléans, Fracia: IRIS Instruments, 8, 2003.

Blay, P.K.: The stratigraphic correlation of the Afram Shales of Ghana, West Africa. Journal of African Earth Sciences 1, 9–16, 1983.

Carney, J., Jordan, C., Thomas, C., & McDonnell, P.: A revised lithostratigraphy and geological map for the Volta Basin, derived from image interpretation and field mapping. In: Kalsbeek, F. (Ed.), The Voltaian Basin, Ghana. Workshop and Excursion, March 10–17, 2008, Abstract Volume. Geological Survey of Denmark and Greenland in Copenhagen, 19–24, 2008.

Carney, J. N., Jordan, C. J., Thomas, C. W., Condon, D. J., Kemp, S. J., & Duodo, J. A.: Lithostratigraphy, sedimentation and evolution of the Volta Basin in Ghana. Precambrian Research, 183, 701-724, doi:10.1016/j.precamres.2010.08.012, 2010.

Christiansen, A. V., & Auken, E.: A global measure for depth of investigation, Geophysics, 77(4), WB171-WB177, doi: 10.4133/1.3614254, 2012.

Crowe, W. A., & Jackson-Hicks, S.: Intrabasin deformation of the Volta Basin, The Voltaian Basin, Ghana Workshop and Excursion, March 10 - 17, 2008, 31 - 38, 2008.

Deynoux, M., Affaton, P., Trompette, R., & Villeneuve, M.: Pan-African tectonic evolution and glacial events registered in Neoproterozoic to Cambrian cratonic and foreland basins of West Africa. *Journal of African Earth Sciences*, *46*(5), pp.397-426, 2006.

Dzikunoo, E., Jørgensen, F., Vignoli, G., Banoeng-Yakubo, B., & Yidana, S. M.: A 3D geological model of the Nasia sub-basin, Northern Ghana - Interpretations from the inversion results of reprocessed GEOTEM data, AEM 2018 / 7th International Workshop on Airborne Electromagnetics Kolding - Denmark, June 17-20, 2018, Abstract 52, 2018.

Eguavoen, I.: The political ecology of household water in Northern Ghana, LIT VerlagMünster, 10, 2008.

FAO: Socio-Economic and Ecological Characteristics. http://www.fao.org/docrep/004/ab388e/ab388e02.htm, last access: 07 October 2019.

Fugro Airborne Surveys: Logistics and Processing Report, Airborne Magnetic and GEOTEM Survey, Areas 1 to 8, Ghana, 92, 2009a.

Fugro Airborne Surveys Interpretation: Airborne Geophysical Survey over the Volta River Basin and Keta Basin Geological Interpretation Summary Report, FCR2350/Job No. 1769, 2009b.

Gaisie, J. S., & Winter, J.: Tillite in the Togo formation in Ghana. Accra, Ghana, 1973.

Geological Survey Department, British Geological Survey; Fugro Airborne Surveys Limited: Radiometric Regolith-landform Interpretation SHEET 1002/1001/100, Mining Sector Support Programme: Project Number 8ACP GH 027/13, 2006.

Goddéris, Y., Donnadieu, Y., Nédélac, A., Dupré, B., Dessert, C., Grard, A., Ramstein, G., & François, L. M.: The Sturtian 'snowball' glaciation: fire and ice, Earth and Planetry Science Letters, 211, doi: 10.1016/S0012-821X(03)00197-3, 1-12, 2003

Gulbrandsen, M. L., Jørgensen, F., Dahlqvist, P., & Persson, L.: A 3D geological soil-modelling workflow using AEM data - A case study from Gotland, Sweden. 7th International Workshop on Airborne Electromagnetics, Kolding - Denmark, June 17 - 20, -p. 4.,2018.

Hoffman, P.F. & Schrag, D.P.: The snowball Earth hypothesis: testing the limits of global change. *Terra nova*, *14*(3), pp.129-155, 2002.

Hoffman, P.F. & Li, Z.X.: A palaeogeographic context for Neoproterozoic glaciation, Palaeogeography, Palaeoclimatology, Palaeoecology, 277(3-4), doi:10.1016/j.palaeo.2009.03.013,158-172, 2009.

575   Høyer, A.-S., Jørgensen, F., Foged, N., He, X., & Christiansen, A. V.: Three-dimensional geological modelling of AEM resistivity data - A comparison of three methods, Journal of Applied Geophysics, 65-78, doi: 10.1016/j.jappgeo.2015.02.005, 2015.

Høyer, A. S., Vignoli, G., Hansen, T. M., Keefer, D. A., & Jørgensen, F.: Multiple-point statistical simulation for hydrogeological models: 3-D training image development and conditioning strategies, Hydrology and Earth System
580   Sciences, 21(12), doi: 10.5194/hess-21-6069-2017, 6069, 2017.

Jessell, M., Boamah, K., Duodu, J. A., & Ley-Cooper, Y.: Geophysical evidence for a major palaeochannel within the Obosum Group of the Volta Basin, Northern Region, Ghana, Journal of African Earth Sciences, 112, 586-596, doi:10.1016/j.jafrearsci.2015.04.007, 2015.

Jordan, C. J., Carney, J. N., Thomas, C. W., McDonnell, P., Turner, P., McManus, K., & McEvoy, F. M.: Ghana Airborne
585   Geophysics Project: BGS Final Report, British Geological Survey Commissioned Report, CR/09/02, 2009.

Jørgensen, F., Møller, R. R., Lars, N., Jensen, N.-P., Christiansen, A. V., & Sandersen, P. B.: A method for cognitive 3D geological voxel modelling of AEM data, Bulletin of Engineering Geology and the Environment, 72(3 - 4), 421-432, doi:10.1007/s10064-013-0487-2, 2013.

Jørgensen, F., Høyer, A.-S., Sandersen, P. B., He, X., & Foged, N.: Combining 3D geological modelling techniques to
590   address variations in geology, data type and density - An example from Southern Denmark, Computers & Geosciences, 81, 53-63, doi:10.1016/j.cageo.2015.04.010, 2015.

Jørgensen, F., Menghini, A., Vignoli, G., Viezzoli, A., Salas, C., Best, M. E., & Pedersen, S. A.: Structural Geology Interpreted from AEM Data-Folded Terrain at the Foothills of Rocky Mountains, British Columbia, 2nd European Airborne Electromagnetics Conference. Malmö, Sweden, September 3 - 7, 2017.

595   Jørgensen, F., & Sandersen, P. B.: Buried and open tunnel valleys in Denmark - erosion beneath multiple ice sheets, Quaternary Science Reviews, 25, 1339 - 1363, doi: 10.1016/j.quascirev.2005.11.006, 2006.

Kalsbeek, F., Frei, D., & Affaton, P.: Constraints on provenance, stratigraphic correlation and structural context of the Volta basin, Ghana, from detrital zircon geochronology: An Amazonian connection? Sedimentary Geology, 86-95, doi: 10.1016/j.sedgeo.2008.10.005, 2008.

600 Kehew, A. E., Piotrowski, J. A., & Jørgensen, F.: Tunnel valleys: Concepts and controversies - A review, Earth Science Review, 113(1 - 2), 33 - 58, doi: 10.1016/j.earscirev.2012.02.002, 2012.

Ley-Cooper, A. Y., Viezzoli, A., Guillemoteau, J., Vignoli , G., Macnae, J., Cox, L., & Munday, T.: Airborne electromagnetic modelling options and their consequences in target definition, Exploration Geophysics, 46, 74-84, doi: 10.1071/eg14045, -2014.

605 Li,Z.-X., Bogdanova, S.V., Collins, A.S., Davidson, A., DeWaele, B., Ernst, R.E., Fitzsimons, I.C.W., Fuck, R.A., Gladkochub, D.P., Jacobs, J., Karlstrom, K.E., Lu, S., Natapov, L.M., Pease, V., Pisarevsky, S.A., Thrane, K., & Vernikovsky, V.: Assembly, configuration, and break-up history of Rodinia: a synthesis. Precambrian Research 160, 179–210, 2008.

Loke, M. H., & Barker, R. D.: Rapid least-squares inversion of apparent resistivity pseudosections by a quasi-Newton 610 method 1, Geophysical prospecting, 44(1), 131-152, doi: 10.1111/j.1365-2478.1996.tb00142.x, 1996.

Loke, M. H.: Rapid 2D resistivity and Iinversion using the least-squares method RES2DINV. Program Manual, 1997.

MacGabhann, B.A.: Age constraints on Precambrian glaciations and the subdivision of Neoproterozoic time, IUGS EdiacaranSubcommission Circular, August 21, 2005.

Meier, P., Kalscheuer, T., Podgorskii, J. E., Kgotlhang, L., Green, A. G., Greenhalgh, S., Rabenstein, L., Doetsch, J., 615 Kinzelbach, W., Auken, E., Mikkelsen, P., Foged, N., Jaba, B.G., Tshoso, G., &Ntibinyane, O.: Hydrogeophysical investigations in the western and north-central Okavango Delta (Botswana) based on helicopter and ground-based transient electromagnetic data and electrical resistance tomography, Geophysics, 79(5), B201-B211, doi: 10.1190/geo2014-0001.1, 2014.

Oldenborger, G. A., Logan, C. E., Hinton, M. J., Sapia , V., Pugin, A. J., Sharpe, D. R., Calderhead, A. I., & Russell, H. A.: 620 3D Hydrogeological Model Building Using Airborne Electromagnetic Data, Near Surface Geoscience 2014-20th European Meeting of Environmental and Engineering Geophysics, Athens - Greece,September, 14 - 18, 2014.

Porter, S.M., Knoll, A.H. and Affaton, P.: Chemostratigraphy of Neoproterozoic cap carbonates from the Volta basin, West Africa, Precambrian Research, 130, 99-112, 2004.

Pryet, A., Ramm, J., Chiles, J.-P., & Auken, E.: 3D resistivity gridding of large AEM datasets: A step tworad enhanced geological interpretation. Journal of Applied Geophysics, no. 2, 277-283, 2011.

Rapiti, A., Jørgensen, F., Menghini, A., Viezzoli, A., & Vignoli, G.: Geological Modelling Implications-Different Inversion Strategies from AEM Data, 24th European Meeting of Environmental and Engineering Geophysics, Porto - Portugal, doi: 10.3997/2214-4609.201802508, 2018.

Ross, M., Parent, M., & Lefebvre, R.: 3D geologic framework models for regional hydrogeology and land-use management: a case study from a Quaternary basin of southwestern Quebec, Canada. Hydrogeology Journal, 13(5-6), 690-707. Doi:10.1007/s10040-004-0365-x, 2005.

Sapia, V., Oldenborger, G. A., Jørgensen, F., Pugin, A. J.-M., Marchetti, M., & Viezzoli, A.: 3D modeling of buried valley geology using airborne electromagnetic data. Interpretation, 3(4), SAC9-SAC22, 2015.

Shields-Zhou, G. A., Deynoux, M., & Och, L.: Chapter 11 The record of Neoproterozoic glaciation in the Taoudéni Basin, NW Africa. Geological Society, London, Memoirs, 36(1), 163–171. https://doi.org/10.1144/m36.11, 2011.

Smith, R., & Annan, P.: The use of B-field measurements in airborne time-domain system: Part I. Benefits of B-field versus dB/dt data. Exploration Geophysics, 24-29, 1998.

Tikhonov, A.N. & Arsenin, V.Y.: Solutions of ill-posed problems, New York, 1977.

Tarantola, A.: Popper, Bayes and the inverse problem. Nature physics, 2(8), 492, https://doi.org/10.1038/nphys375, 2006.

Turner, A. K.: Challenges and trends for geological modelling and visualisation. Bulletin of Engineering Geology and the Environment, 65, 109-127. doi:10.1007/s10064-005-0015-0, 2006.

Van der Vegt, P., Janszen, A., & Moscariello, A.: Tunnel Valleys: Current Knowledge and Future Perspectives. Geological Society, London, Special Publications, 368(1), 75-97, doi: 10.1144/sp368.13, 2012.

Viezzoli, A., Christiansen, A. V., Auken, E., &Sørensen, K.: Quasi-3D modeling of airborne TEM data by spatially constrained inversion. Geophysics, 73(3), F105-F113, https://doi.org/10.1190/1.2895521, 2008.

Viezzoli, A., Munday, T.,AukenT., Auken, E., & Christiansen, A.V.: Accurate quasi 3D versus practical full 3D inversion of AEM data–the Bookpurnong case study. Preview, 149, 23-31, https://doi.org/10.1071/PVv2010n149p23, 2010.

Viezzoli, A., Jørgensen, F., & Sørensen, C.: Flawed processing of airborne EM data affecting hydrogeological interpretation. Groundwater, 51(2), 191-202, https://doi.org/10.1111/j.1745-6584.2012.00958.x, 2013.

650 Vignoli, G., Gervasio, I., Brancatelli, G., Boaga, J., Della Vedova, B., & Cassiani, G.: Frequency-dependent multi-offset phase analysis of surface waves: an example of high-resolution characterization of a riparian aquifer. Geophysical Prospecting, 64, 102-111, 2015.

Vignoli, G., Cassiani, G., Rossi, M., Deiana, R., Boaga, J., &Fabbri, P.: Geophysical characterization of a small pre-Alpine catchment, Journal of Applied Geophysics, 80, 32-42, https://doi.org/10.1016/j.jappgeo.2012.01.007, 2012.

655 Vignoli, G., Fiandaca, G., Christiansen, A. V., Kirkegaard, C., &Auken, E.: Sharp spatially constrained inversion with applications to transient electromagnetic data. Geophysical Prospecting, 63(1), 243-255, doi: 10.1111/1365-2478.12185, 2015.

Vignoli, G., Sapia, V., Menghini, A., &Viezzoli, A.: Examples of improved inversion of different airborne electromagnetic datasets via sharp regularization. Journal of Environmental and Engineering Geophysics, 22(1), 51-61, doi: 660 10.2113/JEEG22.1.51, 2017.

Villeneuve, M., & Cornée, J. J.:Structure, evolution and palaeogeography of the West African craton and bordering belts during the Neoproterozoic.In Precambrian Research (Vol. 69, pp. 307–326). https://doi.org/10.1016/0301-9268(94)90094-9, 1994.

Zhdanov, M.S., Vignoli, G. & Ueda, T.: Sharp boundary inversion in crosswell travel-time tomography. Journal of 665 Geophysics and Engineering, 3, 122-134, 2006.

Zhdanov, M.S.: Inverse theory and applications in geophysics (Vol. 36), Elsevier, 2015.
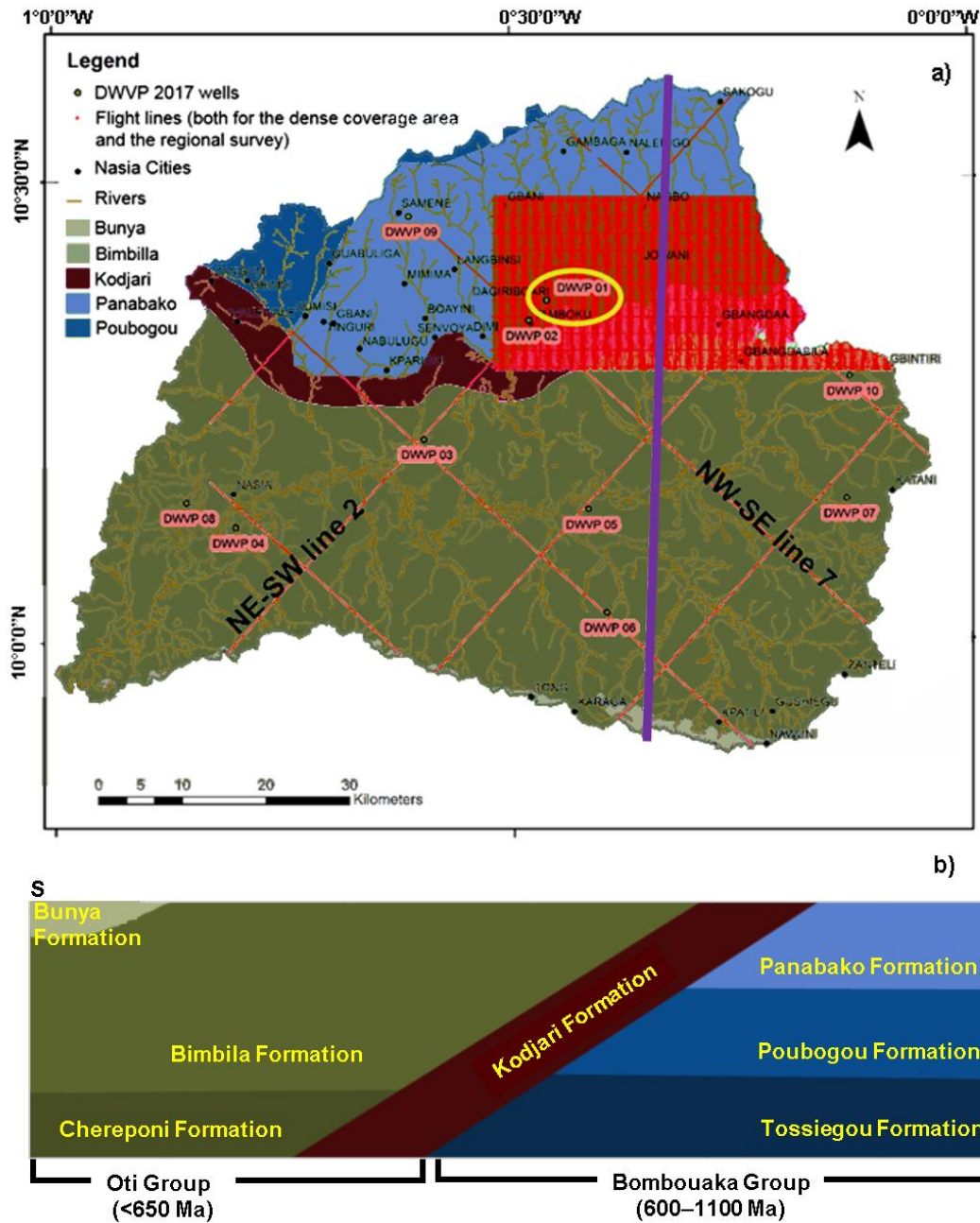
Figure 1: (a) Geologic Map of the Nasia sub-basin after Carney et. al. (2010); the rectangular red area on the top right corner shows the locations of the flight lines of the dense coverage AEM survey (line spacing of 200 m - Fig. 9); the flight lines of the regional survey (20 km by 20 km regular spacing) are shown as red lines (two of them are indicated with "NE-SW line 2" and "NW-SE line 7"). (b) Conceptual Model of the geology along a cross sectional N-S line within the study area - (solid blue violet line in the panel (a). The age determinations for Oti and Bombouaka Groups are those reported in Kalsbeek et al. (2008).
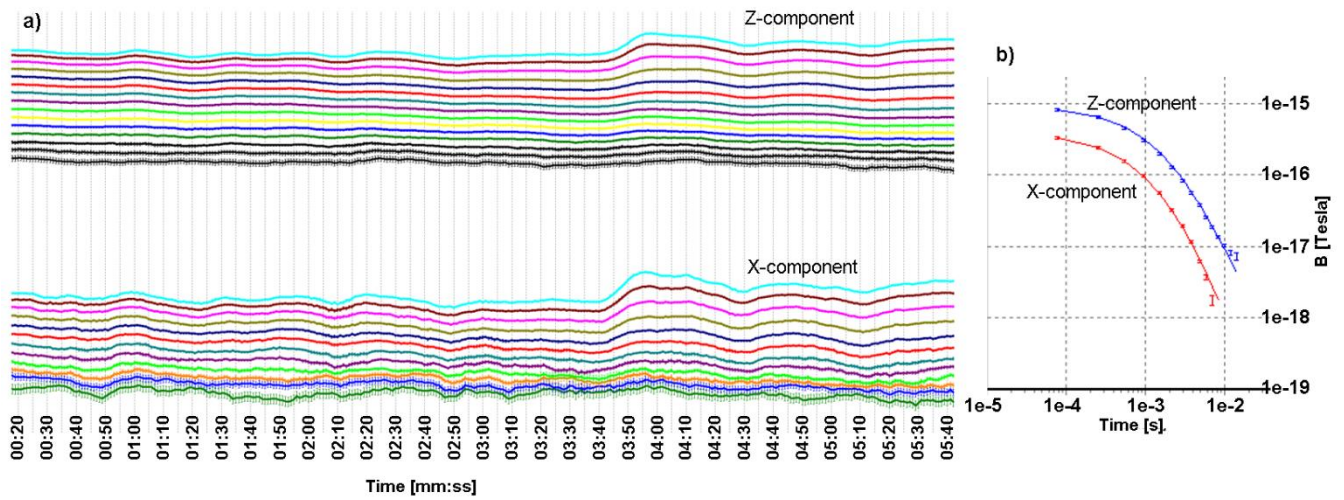
675   **Figure 2:** (a) An example of the Z and X components of the B-field data obtained after the application of the moving window stacking with width varying with the time-gates. (b) Example of a typical sounding (Z and X components): the vertical bars represent the stacked data with the associated uncertainty; the solid lines are the calculated data corresponding to the inversion model (not shown).
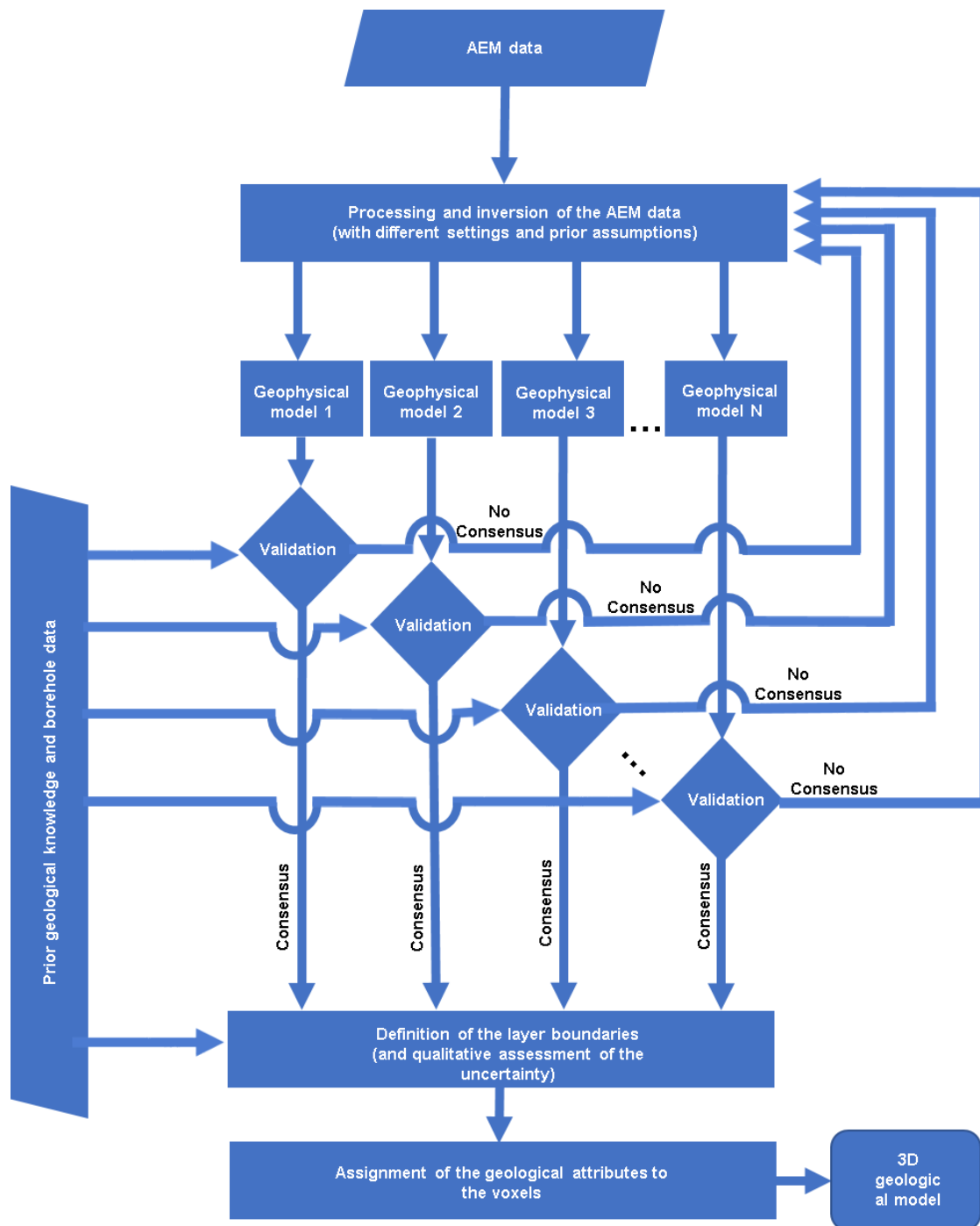
680

Figure 3: The workflow describing the iterative interaction between geologists and geophysicists leading to the development of the 3D geological model ~~integrating consistently synthetizing, in a coherent way,~~ all the diverse pieces of information available (geophysical data, prior geological knowledge, wells, etc.).
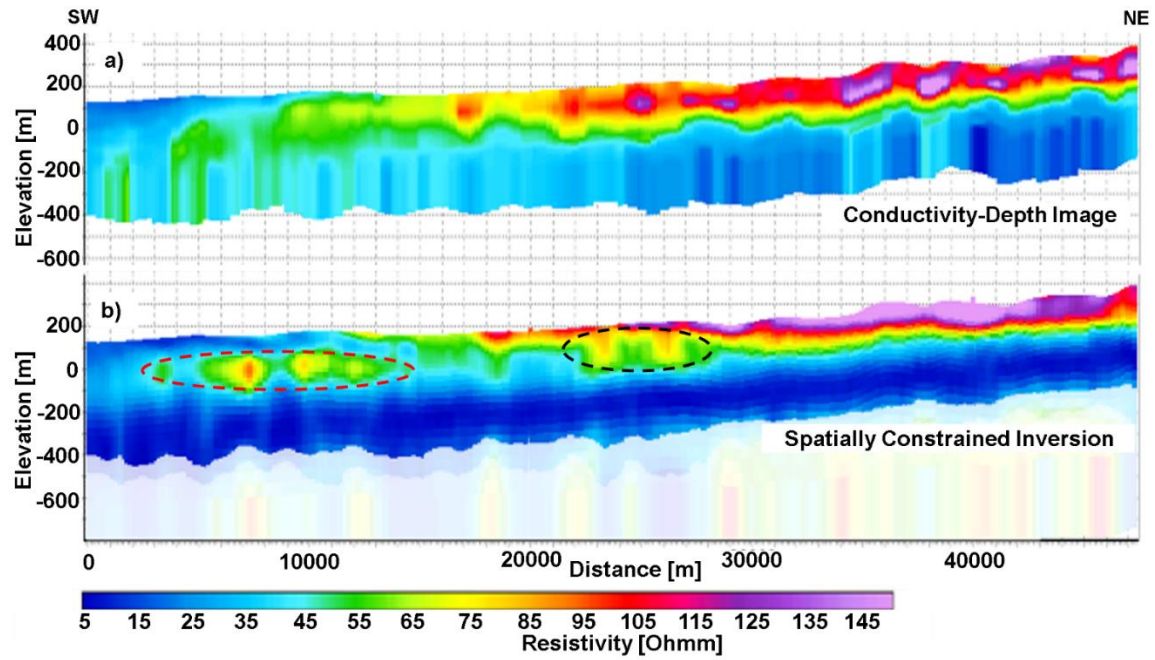
Figure 4: (a) The original Conductivity-Depth Image (CDI) ~~along~~ in a portion of NE-SW line 2 (Fig. ~~1~~1a); (b) the associated result obtained with the new data processing and inversion approach (smooth Spatially Constrained Inversion).

690
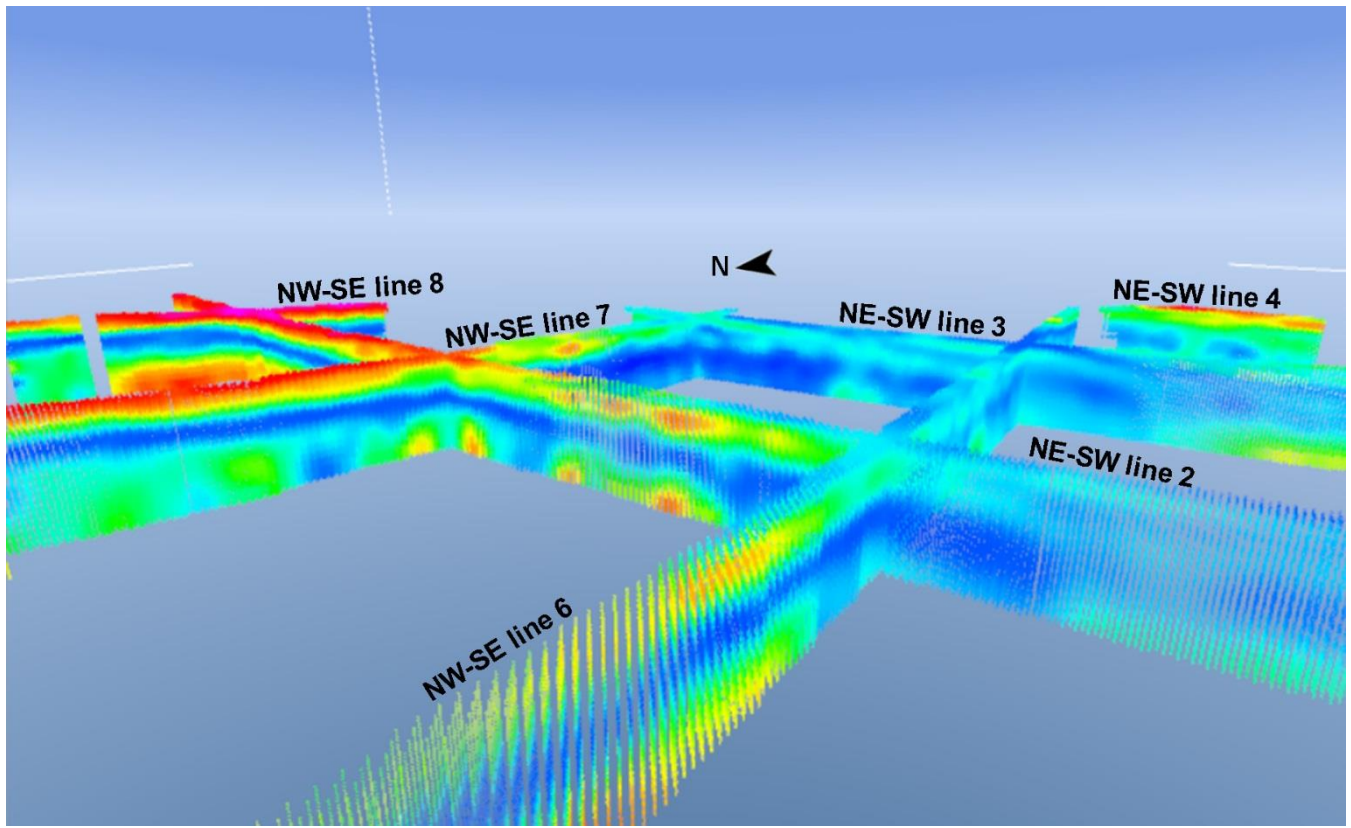
Figure 5: A 3D view of the B-field SCI results along the 20km x 20km grid lines in the study area. These soundings were used as basis for geologic interpretation and modelling. The arrowhead points northwards. For the locations of the grid lines, see Fig. 1a.
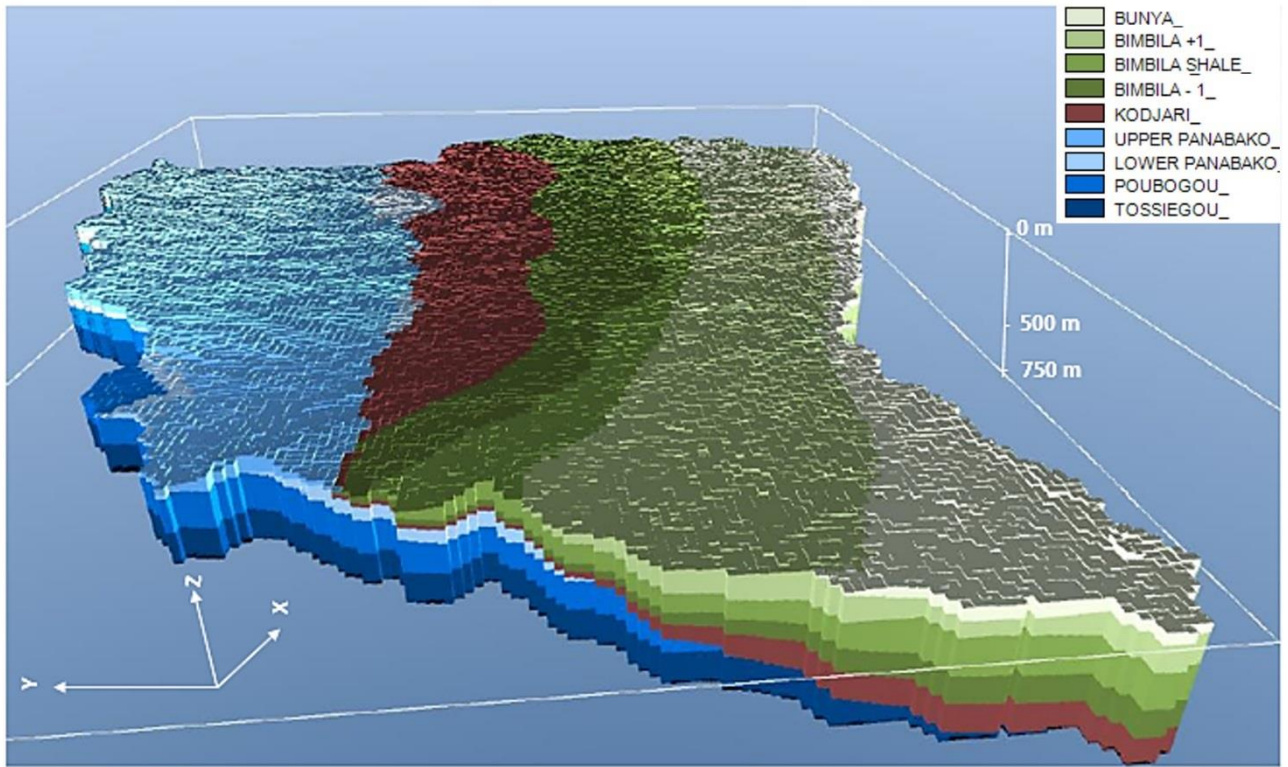
695   **Figure 6: 3D geological model of the Nasia sub-basin resulting from the combined interpretation of the B-field airborne data, the prior geological knowledge of the area, and the available wells.**
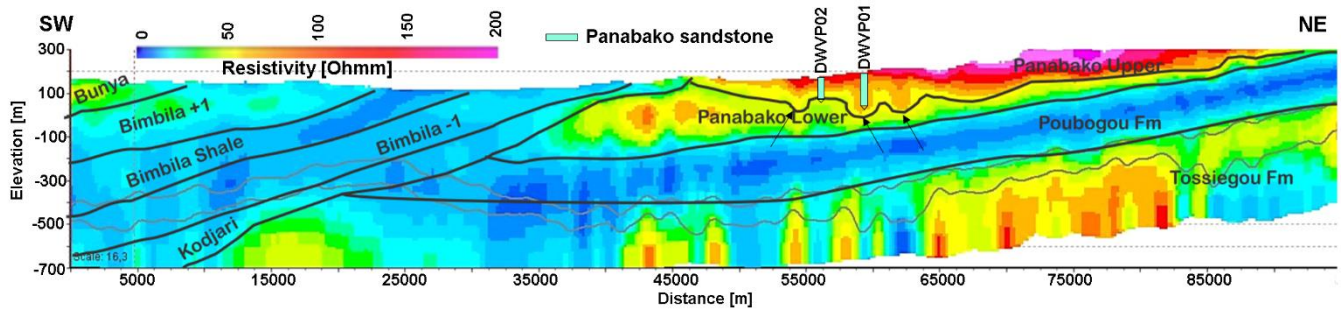
Figure 7: ~~a.)~~ Cross-section ~~from the Northeast~~ along SW-NE line 2 ~~of~~ across the study area (see Fig. ~~11~~1a for the location) with the conceptual geological interpretations showing the U-shaped valleys (~~between~~ between ~ ~~125 and ~135~~53 and 63 km, whose location is indicated by three black arrows). ~~b.) Cross-section from the Northeast along SW-NE line 2 of the study~~In addition, also two of the ~~area showing some~~ geologic logs (DWVP02 and DWVP01 – Fig. 1a) used ~~in the~~for –demarcation of lithostratigraphic boundaries and the interpretation/verification of the geophysical model are shown. The two solid grey lines at the bottom represent the DOIs.
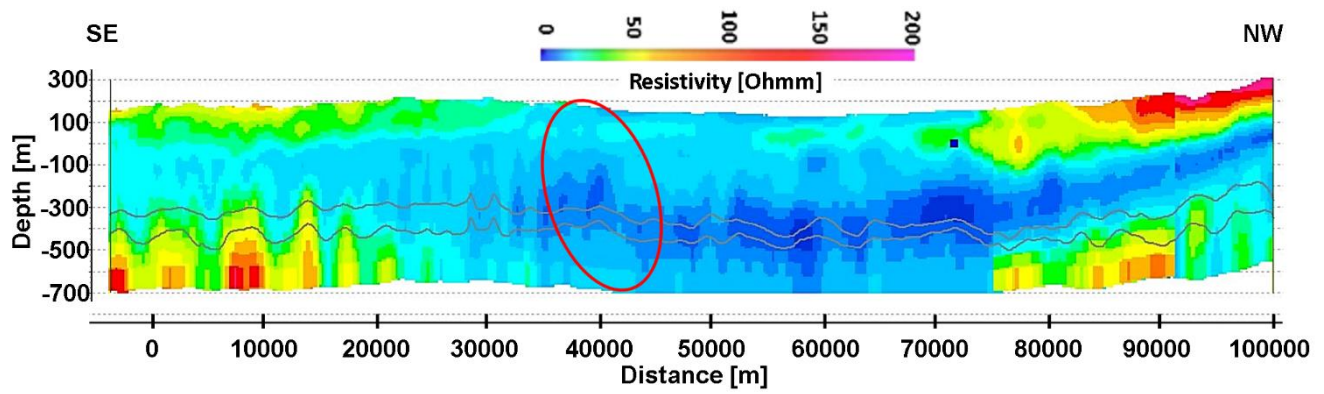
Figure 8: Cross-section along NW-SE line 7 (Fig. ~~1~~1a) showing faulting (within the red circle) in the Bimbila. The DOI is ~~showed~~ shown as a solid grey line (there are two of them accordingly to their definition – more details on this distinction can be found in Christiansen and Auken, 2012).

710
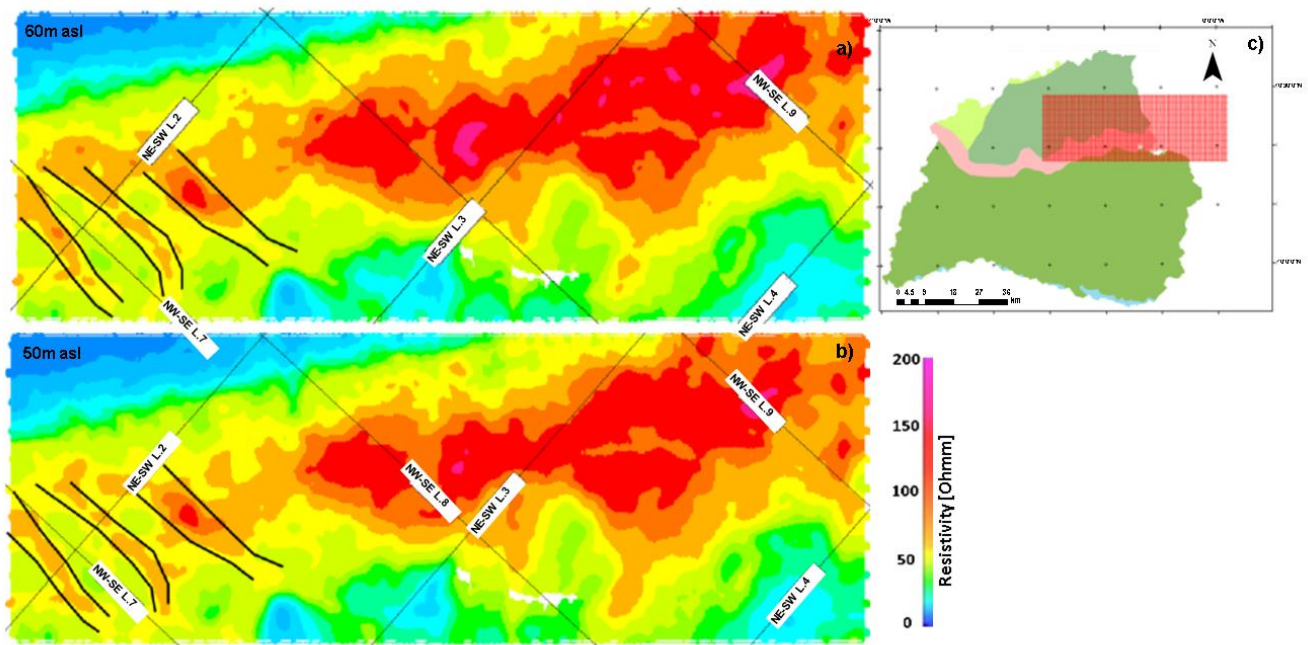
Figure 9: Horizontal resistivity slices at 60m (a) and 50 m (b) depth of the portion of the study area - in red, in the panel (c) - characterized by a geophysical sampling much denser (200 m line-spacing) than the regional survey - in this respect, see the lines from "NE-SW L.2" to "NW-SE L.9" in panel (a) and (b) characterized by a 20 km ~~by~~x 20 km spacing (Fig. 1a). The black solid lines in the left-bottom corner of panels (a) and (b) show the location of the paleovalleys discussed in the manuscript. Hence, the features interpreted as paleovalleys can be identified in both the two independently inverted datasets (i.e. the dense coverage area and the regional survey). Clearly, the densely sampled data can provide further insights in terms of spatial coherency of the paleovalleys' NW-SE trend.

715